

# **AN ASPECT OF THE DYNAMICS OF MECHANICAL FACE SEALS**

*by*

LIEUTENANT K A J PINTO

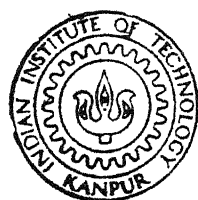
ME  
K392

TH  
ME/1992/M  
P 658a

M

IN

ASP



DEPARTMENT OF MECHANICAL ENGINEERING  
**IAN INSTITUTE OF TECHNOLOGY KANPUR**  
JANUARY, 1992

# **An Aspect of the Dynamics of Mechanical Face Seals**

**A Thesis Submitted  
in Partial Fulfilment of the  
Requirements for the Degree  
of MASTER OF TECHNOLOGY**

*by*

**Lieutenant K A J Pinto**

*to the*

**DEPARTMENT OF MECHANICAL ENGINEERING  
INDIAN INSTITUE OF TECHNOLOGY KANPUR  
JANUARY, 1992**

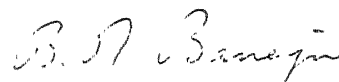
ME-1882-M-PIN

PIN-A

ME-1882-M-PIN - A.S.P.

CERTIFICATE

This is to certify that the thesis entitled, "An Aspect of the Dynamics of Mechanical Face Seals" by Lt. K.A.J. Pinto is a record of the work carried out under my supervision and has not been submitted elsewhere for a degree.



Dated 23 Jan. 1992

Dr. B.N. Banerjee

Assistant Professor

Department of Mechanical Engg.  
Indian Institute of Technology  
Kanpur - 208016

## **ACKNOWLEDGEMENT**

I owe deep gratitude to Dr. B.N. Banerjee for his inspiring and invaluable guidance to this thesis work. I would also like to thank Dr. M.M. Oberai for his interest and help in sorting out some of the mathematical intricacies of this thesis.

It is also a pleasure to acknowledge, the dedication of the faculty at the Department of Mechanical Engineering, and the excellent computing and reference facilities made available by this Institute.

Finally, I thank my wife for her patience and understanding during my Masters Programme.

**Kevin Pinto**

## ABSTRACT

Considering relative misalignment between the seal faces to be the basis of pressure generation and sealing, it is investigated whether hydrodynamic and squeeze film pressures provide stable seal operation. The motion of the flexibly mounted stator ring in response to the rotation of the rotor ring consists of a wobble. It is described by two non-linear differential equations for two mutually perpendicular components of the net tilt of the stator. The equations are reduced to linear form by assuming constant wobble frequency and conditions are found for the tilt to increase, decrease or remain constant. A relationship between the wobble frequency of the stator ring and the frequency of rotation of the rotor ring in terms of the support stiffness, moment of inertia and mean radius of the stator ring is established.

It is found that when the condition for constant tilt is satisfied the wobble frequency of the stator ring is one-half of the shaft or rotating ring frequency. This state results in zero fluid film moments, causing failure of the seal. The relationship between frequency of rotation of the rotor and the support stiffness, moment of inertia and mean radius of the seal provide a means for the designer to avoid this mode of seal failure.

1512-1929

TEXAS STATE LIBRARY

113081

Considering relative misalignment between the seal faces to be the basis of pressure generation and sealing, it is investigated whether hydrodynamic and squeeze film pressures provide stable seal operation. The motion of the flexibly mounted stator ring in response to the rotation of the rotor ring consists of a wobble. It is described by two non-linear differential equations for two mutually perpendicular components of the net tilt of the stator. The equations are reduced to linear form by assuming constant wobble frequency and conditions are found for the tilt to increase, decrease or remain constant. A relationship between the wobble frequency of the stator ring and the frequency of rotation of the rotor ring in terms of the support stiffness, moment of inertia and mean radius of the stator ring is established.

It is found that when the condition for constant tilt is satisfied the wobble frequency of the stator ring is one-half of the shaft or rotating ring frequency. This state results in zero fluid film moments, causing failure of the seal. The relationship between frequency of rotation of the rotor and the support stiffness, moment of inertia and mean radius of the seal provide a means for the designer to avoid this mode of seal failure.

$$\text{The critical condition to avoid is } \omega = C \sqrt{\frac{kr_m^2}{I_0}} \text{ where } r_m$$

is the mean radius of the seal ring,  $I_0$  its transverse moment of inertia , k a measure of its support stiffness and c a constant of proportionality determined by the manner in which the support stiffness is modelled.

## List of Figures

	Page No
1.1 A low-cost volume-production mechanical seal (Crane Packing Ltd., Type 25A)	02
1.2 Hydrodynamic film pressure generation due to relative face misalignment	06
1.3 Mathematical model of the face seal	09
1.4 The misaligned face seal	11
1.5 Hydrodynamic film pressure comparison	25
1.6 Squeeze film pressure comparison	26
1.7 Hydrodynamic film pressure distribution with and without large sealed pressure	28
1.8 Film pressure distribution	29
1.9 Hydrodynamic and squeeze moments acting on the stator ring	30
2.1 Coordinate system	33
2.2 Model for film thickness	38
2.3 Model for calculating moments	40
2.4 Model for the Bellows	45
2.5(a) Model for spring displacements	45
2.5(b) Free body diagram of the stator ring showing spring forces	45
3.1 Signals showing a wobble frequency approximately half the frequency of rotation [5]	58

## NOMENCLATURE

$h$	local film thickness; seal gap height
$\bar{h}$	mean film thickness
$\cdot \bar{h}$	axial velocity due to change in mean film thickness
$I$	moment of inertia
$\hat{i}, \hat{j}, \hat{k}$	unit vectors in the directions of the positive x,y and z axes.
$k$	spring stiffness
$l$	uncompressed length of spring
$M$	moment
$O$	geometric centre of the stator ring
$p$	pressure
$r$	radius; or cylindrical coordinate
$t$	time
$X, Y, Z$	inertial reference frame axes
$x, y, z$	rotating reference frame axes
$\gamma$	relative angular misalignment (tilt) between seal faces
$\dot{\gamma}$	tilting angular velocity
$\Delta$	spring displacement
$\delta$	initial spring compression
$\varepsilon$	tilt parameter, $\gamma r_m / \bar{h}$
$\theta$	cylindrical coordinate; angular displacement around seal ring measured from the positive y axis
$\mu$	viscosity

$\phi$  angular displacement around seal ring measured from the positive Y axis

$\psi$  Euler angle specifying the position of the x,y axes with reference to the X,Y axes in the horizontal plane

$\dot{\psi}$  wobble frequency

$\omega$  rotor (shaft) angular velocity

$\vec{\omega}$  absolute angular velocity of the x-y-z rotating reference frame

$\vec{\Omega}$  absolute angular velocity of the stator ring

### Subscripts

hyd hydrodynamic

i inner radius

m mean radius

o outer radius

s sealed fluid

sp spring

X,Y,Z inertial reference frame axes

x,y,z rotating reference frame axes

xx,yy,zz indicate principal axes of the stator ring

## CONTENTS

Page No.

ABSTRACT	i
LIST OF FIGURES	iii
NOMENCLATURE	iv
CHAPTER 1	
1.1    Introduction	01
1.2    The mechanical face seal model	10
1.3    The development of film pressures	12
1.4    Hydrodynamic effect	14
1.5    Squeeze	17
1.6    Approximation	19
1.7    Hydrodynamic effect with approximation	19
1.8    Squeeze effect with approximation	21
1.9    Comparison of results from the complete and approximate equations for pressure	23
1.10   Results	27
1.11   Combined effect of film forces	27
CHAPTER 2	
2.1    Dynamics of the mechanical face seal	32
2.2    The coordinate system	32
2.3    Moment of momentum equations	35
2.4    Fluid film generated moments	37
2.5    Moments due to the bellows	46
2.6    The equations of motion	48
CONCLUSIONS	57
APPENDIX A	62
APPENDIX B	71
APPENDIX C	73

## CONTENTS

	Page No.
ABSTRACT	i
LIST OF FIGURES	iii
NOMENCLATURE	iv
CHAPTER 1	
1.1    Introduction	01
1.2    The mechanical face seal model	10
1.3    The development of film pressures	12
1.4    Hydrodynamic effect	14
1.5    Squeeze	17
1.6    Approximation	19
1.7    Hydrodynamic effect with approximation	19
1.8    Squeeze effect with approximation	21
1.9    Comparison of results from the complete and approximate equations for pressure	23
1.10   Results	27
1.11   Combined effect of film forces	27
CHAPTER 2	
2.1    Dynamics of the mechanical face seal	32
2.2    The coordinate system	32
2.3    Moment of momentum equations	35
2.4    Fluid film generated moments	37
2.5    Moments due to the bellows	46
2.6    The equations of motion	48
CHAPTER 3	
3.1    Main results	57
CONCLUSIONS	62
APPENDIX A	63
APPENDIX B	71
APPENDIX C	73
REFERENCES	76

### 1.1 Introduction

A large number of seals of different types are used in Industry, for fluid sealing in systems with rotating shafts. The mechanical seal, as compared to simpler stuffing boxes and gland packings used for rotating shafts, has the advantage of smaller leakage losses, reduced maintenance and longer life due to no wear. The function of a seal is to separate pressurized fluids where, for instance, a moving shaft passes through a machine housing or passes from one part of the machine to another. It may also serve to prevent entry of foreign bodies into an operating medium or the loss of lubricant from bearings and transmissions. A typical low-cost volume-production face seal is illustrated in Figure 1.1. This type of seal is used in such applications as motorcar water pumps, domestic washing machines, and small centrifugal pumps. Very often the floating member is stationary, running against the end of the pump impeller for instance. The high pressure region is on the outside of the seal, causing a leakage path as indicated. The mechanical seal restricts leakage of fluid in the radial direction, between the nominally plane sealing surfaces of the stator ring and the impeller. The floating stator ring is typically of a moulded resin material. The case is a one-piece pressed - steel ring within which a rubber bellows is fitted and retained by its own initial interference or a combination of this and the axial thrust of the face-loading spring.

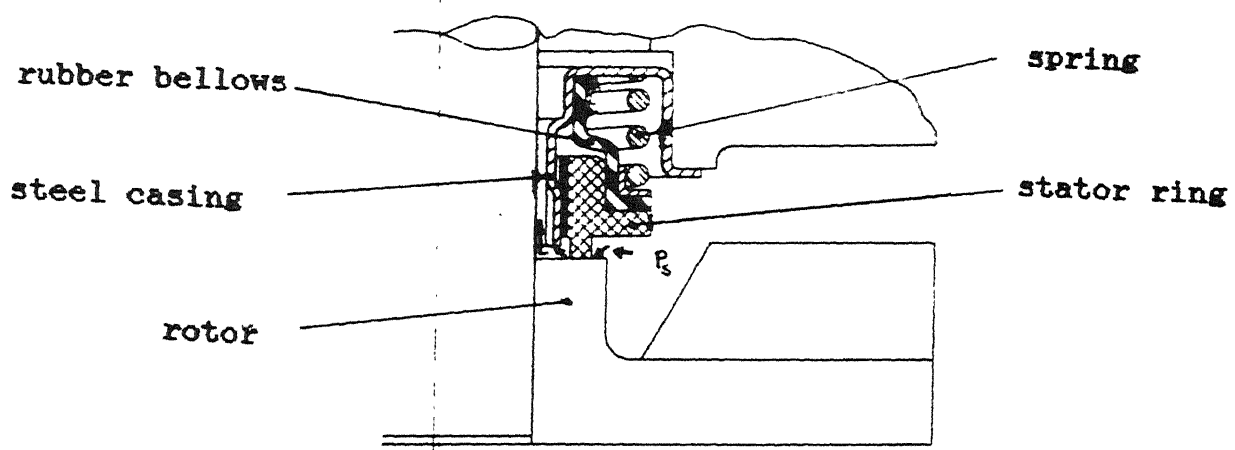


**Fig. 1.1** A low-cost volume-production mechanical seal  
(Crane Packing Ltd., Type 25A)

Mechanical seals, also known as radial face seals, have many applications. In the engineering Industry, they serve to seal crank shafts, water pumps and auxiliary pumps in automobiles, power generating systems and marine engines. They are also common in water turbines, boiler feed pumps compressors and high pressure rotary pumps. In aircraft and rockets, they are used for sealing gas turbine shafts, turbo-super chargers, hydraulic units and booster pumps for fuel and liquid gas. The fluids sealed include liquidoxygen, super heated water, solutions such as brewing liquors, dyes, sludge, various acids, hydro-carbons, asphalts, cocoa, plastics, radioactive gases and liquids. For various applications, suitable seal materials and special designs are used for chemical, mechanical and thermal compatibility. Pressures ranging from high vacuum ( $10^{-5}$  torr upto 200 bar) shaft speeds upto 50,000 rpm and temperatures from  $-200^{\circ}\text{C}$  upto  $450^{\circ}\text{C}$  are some of the requirements.

The stability of the seal operation is a crucial factor in order that the seal faces may not come into direct contact. Such contact can lead to frictional overheating and severe thermal distortion of the seal faces following which the seal fails.

In addition, the following factors have an important influence on leakage losses, life and reliability.

1. The width of the seal.
2. The sliding speed.

3. The surface roughness and the waviness of the sliding surfaces.
4. The temperature of the sealed liquid and the sliding surfaces, especially any variation with time.
5. The shape of the interface profile. This is dependent upon mechanical and thermal distortions which can occur during operation.
6. The choice of seal face materials.
7. The sealed medium, its degree of solid contamination and its chemical behaviour.
8. Oscillations, side loads, interrupted operation, periodic dry running, heating and cooling cycles, the direction of the radial flow leakage, eccentric running and other factors determined by design on operating conditions, especially those affecting heat transfer characteristics.

In Mechanical seals used under high loads, or where the sealing fluid has an inadequate lubricating ability, pressurized fluid is pumped into the seal interface.

Successful operation of the mechanical seal in order to reduce wear and maintain the integrity of the sealing surfaces, primarily requires that the faces must remain separated by a lubricating film throughout seal operation. Also, to minimize leakage, the seal - gap must be extremely small, of the order of  $10^{-6}$  mm.

Reference [1] shows that a lubricating film can exist between the seal faces. The paper also provides an insight into the mechanisms of successful seal operation. The mechanisms responsible for the development of the lubricating film pressure that acts to separate the faces of the seal, include angular misalignment, surface waviness including thermal deformation effects, surface asperities and axial vibration.

Stanghan - Batch and Iny [2] applied the hydrodynamic theory of lubrication to calculate film pressure in an idealized wavy faced seal. The pressures were found to be sufficient for supporting the applied face load. On the basis of their results, Stanghan - Batch and Iny postulated that successful operation of a face seal depends on the generation of a hydrodynamic film between the seal faces. The film not only prevents direct contact between the two faces, but also provides the sealing pressure. The authors went on to suggest that the performance of mechanical seals can be improved by giving one face an appropriately wavy surface at the time of manufacture.

An angular misalignment (tilt) is akin to a single lobed waviness.

In this thesis, relative angular misalignment of the seal faces is considered as a possible mechanism for fluid film lubrication and for the development of the lubricating film

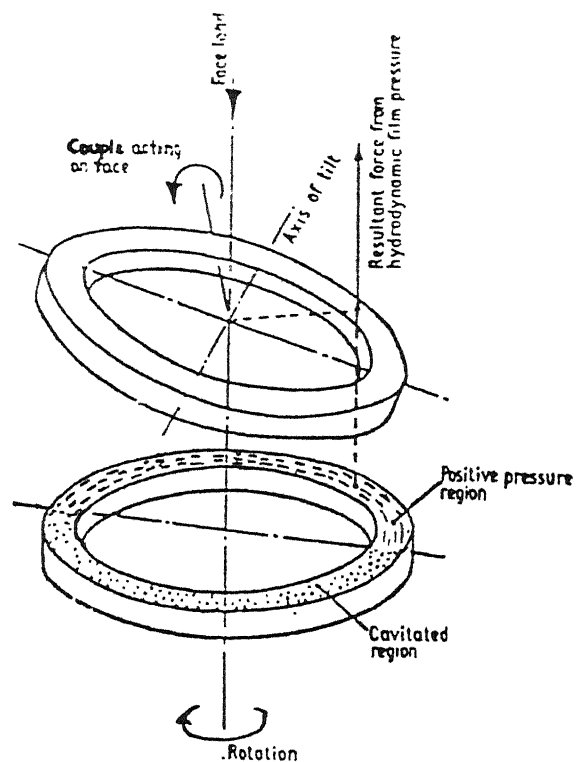


Fig. 1.2. Hydrodynamic film pressure generation due to relative face misalignment [2]

pressure at the seal interface. Equations for film pressures dependent on system parameters and seal geometry are derived. A model of the mechanical seal is considered, with one face rigidly mounted and the other with a floating and flexible mounting, with the object of analysing the dynamics and stability of the seal.

Stanghan - Batch and Iny's theory of face seal operation [2], envisages only a hydrodynamic film and hydrodynamic pressure. Since the hydrodynamic pressure is generated by a fluid film of varying thickness around the seal circumference, a hydrodynamically induced moment acts on the seal face. The effect of this moment is to neutralize the relative face inclination if such inclination consists of a single - lobed waviness of the seal face. A two - lobed waviness, on the other hand, generates a two-lobed hydrodynamic pressure which can produce a net zero moment and sustain the film conditions. Thus Stanghan - Batch and Iny were forced to suggest that the hydrodynamic action in a face seal can work only when a two - lobed waviness exists, ruling out the possibility of a relative angular misalignment as the origin of the hydrodynamic pressure.

Figure 1.2 illustrates the action of the hydrodynamic moment and shows how it neutralizes the face tilt. In practice, the seal faces are carefully lapped before installation. The flexible mounting of one face of the seal however permits it to tilt, thereby generating a film with a varying thickness (single -

lobed wave). Any theory of face-seal operation should consider the possibility of hydrodynamic effects arising out of a relative angular misalignment and the conditions for the dynamic stability of such a configuration.

The couple generated by pure hydrodynamic pressure tends to neutralize the relative tilt and establish parallelity of the two faces. In this process, fluid is squeezed out of the thicker regions of the fluid film. That, in turn, generates a squeeze film pressure which resists the hydrodynamic moment. Thus if hydrodynamic pressure can disturb the tilt configuration the squeeze film pressure may restore it.

The objective of this thesis was to investigate whether hydrodynamically generated film pressure and squeeze film pressure provide stable seal operation. Therefore a simplified model of a mechanical seal is chosen, considering only the relative misalignment between the seal faces as the mechanism of pressure generation and sealing. A more complete model would include surface - waviness, axial vibration and the effect of the support arrangements. For axial vibration to take place the mean film thickness has to be time dependent. Support arrangement effects would have to take into account the flexibility of the seal faces due to the presence of rubber gaskets and O-rings. The damping characteristics of the support arrangement would also have to be considered. In this first study, such effects are neglected.

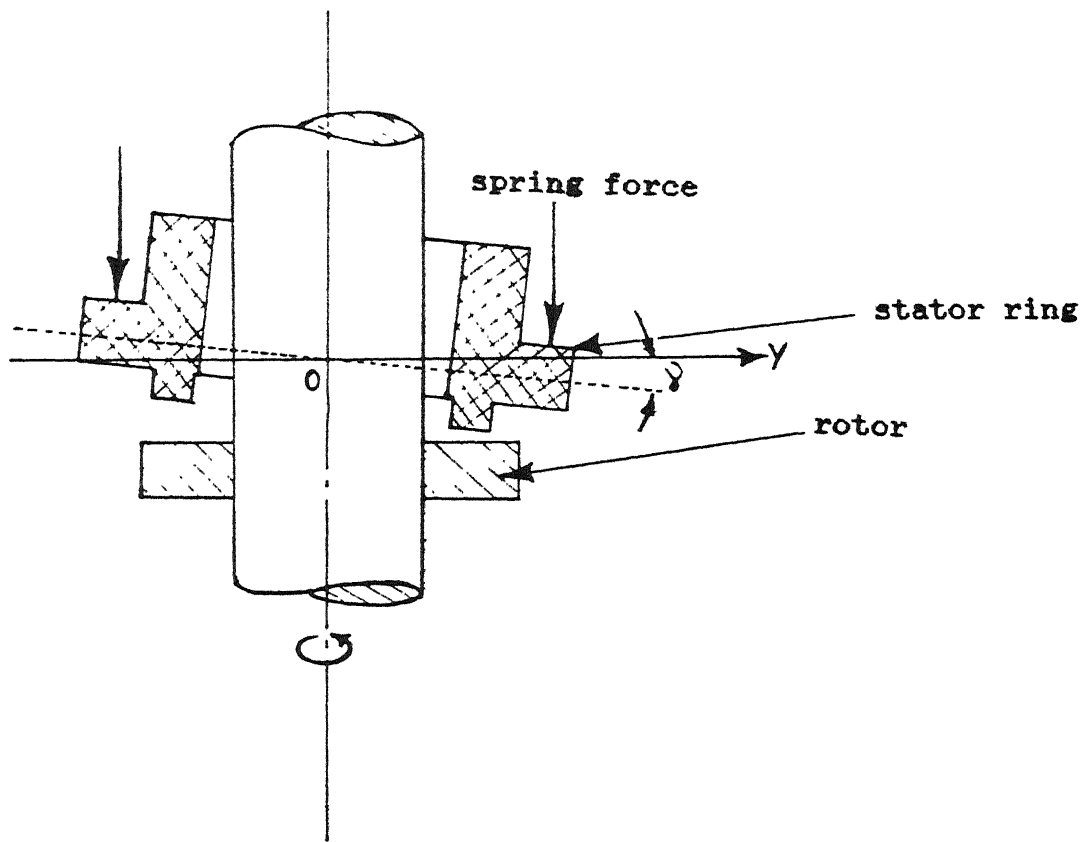


Fig. 1.3 Mathematical model of the face seal

## 1.2 The Mechanical Face Seal Model

A simple mechanical face seal configuration is shown in figure 1.1. Here the rotating seat is rigidly mounted on the shaft, with no axial translating freedom and with perfect alignment.

The stationary ring (stator) is flexibly mounted on a spring. Therefore the stator can undergo both axial translation and tilt. The tilt can be looked upon as two rotations about mutually perpendicular diameters of the stator.

Both faces are flat. The shaft has constant angular velocity. The lubricating film pressure that acts to separate the faces of the seal is developed because of the seal ring angular misalignment. The mathematical model of the mechanical face seal with a misaligned seal ring is shown in Figure 1.3. The seal ring angular misalignment creates a convergent and divergent region in the intervening fluid film.

The principle of hydrodynamic lubrication is responsible for the film pressure development.

In addition to the tangential motion causing hydrodynamic lubrication, the stator - ring can also have a motion normal to the surface of the rotor. This motion also helps in development of a film pressure and the principle is known as squeeze film lubrication.

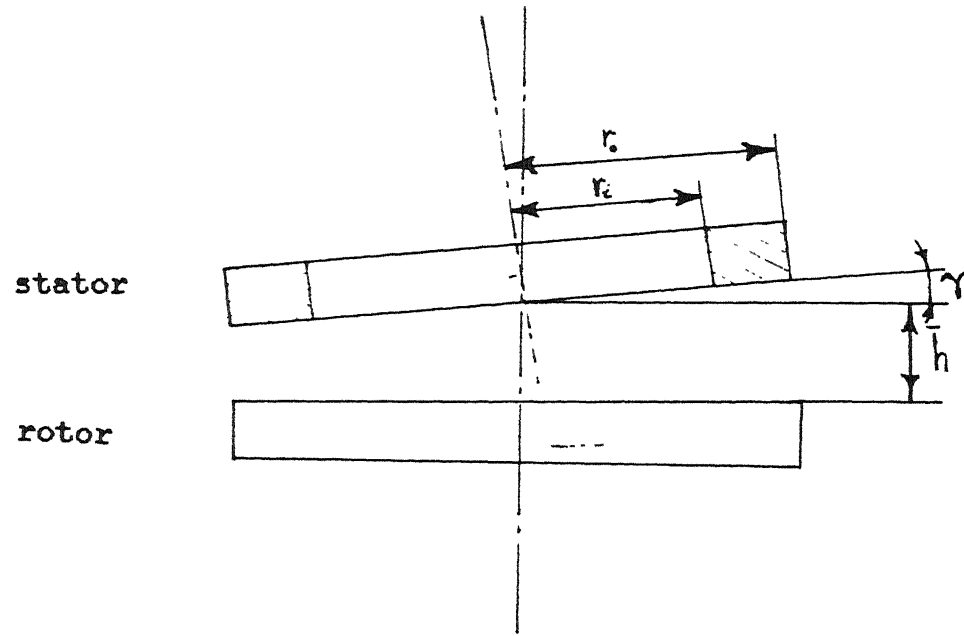


Fig. 1.4 The misaligned face seal

### 1.3 The Development of Film Pressures

The variation of film pressure in a mechanical seal is described by the Reynolds equation. The following assumptions are inherent in the use of the Reynolds equation:

- 1) the fluid is incompressible and the flow is laminar,
- 2) the fluid properties remain constant i.e. effects due to variation in temperature and pressure are neglected,
- 3) inertial effects are negligible,
- 4) the solid bodies remain rigid,
- 5) the film is of sufficiently small thickness that the fluid pressure can be considered constant though the thickness of the film,
- 6) the radius ratio  $r_i/r_o$  (fig. 1.4) is of the order 1, i.e. the face width is small compared to the mean radius of the seal. The simplified Reynolds equation for short bearings, using cylindrical co-ordinates is,

$$\frac{1}{r} \frac{\partial}{\partial r} (h^3 r \frac{\partial p}{\partial r}) = 6 \mu (\omega \frac{dh}{d\theta} + 2 \frac{dh}{dt}) \quad (1.1)$$

The film thickness  $h$  is given by (refer Fig. 1.4),

$$h = \bar{h} + \gamma r \cos \theta \quad (1.2)$$

where  $\theta$  is measured from the location of the maximum film thickness.

Then,

$$\frac{dh}{d\theta} = -\gamma r \sin \theta \quad (1.3)$$

If the film thickness is measured in a moving reference frame, then  $\dot{\theta}$  is zero, as the time derivative of theta i.e.  $\dot{\theta}$  is the angular velocity of the reference frame which will not be seen in the same reference frame.

Therefore,

$$\frac{dh}{dt} = \dot{h} + \dot{\gamma}r \cos \theta \quad (1.4)$$

Substituting equations (1.3) and (1.4) in (1.1),

$$\frac{1}{r} \left[ \frac{\partial}{\partial r} \left( h^3 r \frac{\partial p}{\partial r} \right) \right] = -6\mu\omega r \sin \theta + 12\mu \dot{h} + 12\mu \dot{\gamma} r \cos \theta$$

i.e

$$\frac{1}{r} \left[ \frac{\partial}{\partial r} \left( h^3 r \frac{\partial p}{\partial r} \right) \right] = -6\mu\omega r \sin \theta \omega + 12\mu (\dot{h} + \dot{\gamma} r \cos \theta) \quad (1.5)$$

On the right hand side of equation (1.5), the first term represents hydrodynamic effects due to  $\omega$  and the second term represents squeeze effect due to  $\dot{\gamma}$  and  $\dot{h}$ .

#### 1.4 Hydrodynamic Effect

As equation (1.5) is linear, the pressure distribution for only the hydrodynamic effect is given by

$$\frac{1}{r} \left[ \frac{\partial}{\partial r} \left( h^3 r \frac{\partial p}{\partial r} \right) \right] = -6\mu\gamma r \sin \theta \omega \quad (1.6)$$

$$\text{i.e. } \frac{\partial}{\partial r} \left( h^3 r \frac{\partial p}{\partial r} \right) = -6\mu\omega\gamma r^2 \sin \theta \quad (1.7)$$

Integrating once with respect to 'r'

$$(h^3 r \frac{\partial p}{\partial r}) = -6\mu\omega\gamma r \sin \theta - \frac{r^3}{3} + C_1$$

$$\text{i.e. } \frac{\partial p}{\partial r} = \frac{-2\mu\omega\gamma \sin \theta r^2}{h^3} + \frac{C_1}{h^3 r} \quad (1.8)$$

Substituting for  $h$  from (1.2) into (1.8)

$$\frac{\partial p}{\partial r} = \frac{-2\mu\omega\gamma \sin \theta r^2}{(\bar{h} + \gamma r \cos \theta)^3} + \frac{C_1}{(\bar{h} + \gamma r \cos \theta)^3 r}$$

$$= \frac{-2\mu\omega\gamma \sin \theta r^2}{\bar{h}^3 (1 + \frac{r \cos \theta r}{\bar{h}})^3} + \frac{C_1}{\bar{h}^3} \frac{1}{r(1 + \frac{r \cos \theta r}{\bar{h}})^3}$$

Integrating with respect to 'r' using tables to integration [3]

$$p = \frac{-2\mu\omega r \sin\theta}{h^3} \frac{\bar{h}^3}{r^3 \cos^3\theta} \left[ \ln \left( 1 + \frac{r \cos\theta}{\bar{h}} \right) + \frac{2}{1 + r \cos\theta/\bar{h}} - \frac{1}{2(1 + r \cos\theta/\bar{h})^2} \right]$$

$$+ \frac{C_1}{h^3} \left[ \frac{1}{2} \left( \frac{2 + r \cos\theta/\bar{h}}{1 + r \cos\theta/\bar{h}} \right)^2 + \ln \left( \frac{r}{1 + r \cos\theta/\bar{h}} \right) \right] + C_2$$

where  $C_1$  and  $C_2$  are constants of integration

Simplifying,

$$p = \frac{-2\mu\omega r \sin\theta}{r^3 \cos^3\theta} \left[ \ln \left( 1 + \frac{r \cos\theta}{\bar{h}} \right) + \frac{2}{1 + r \cos\theta/\bar{h}} - \frac{1}{2} (1 - 2r \cos\theta/\bar{h}) \right]$$

$$+ \frac{C_1}{h^3} \left[ 2 \left( \frac{1 + r \cos\theta/\bar{h}}{1 + r \cos\theta/\bar{h}} \right)^2 + \ln \left( \frac{r}{1 + r \cos\theta/\bar{h}} \right) \right] + C_2 \quad (1.8)$$

In order to find the constants of integration  $C_1$  and  $C_2$ , boundary conditions have to be utilized, at the inner and outer radius of the seal.

The choice of having the sealed fluid placed on the inside of the sealing ring for an 'inside-seal' or on the outside of the sealing ring for an 'outside-seal', should be made to suit both

seal-leakage, as well as duty requirements. The disposition of the sealed fluid on the inside or outside of the seal is likely to have a strong impact on seal performance. Centrifugal action due to seal rotation tends to fling the interfacial fluid outwards. The radial variation of the hydrostatic pressure tends to drive the fluid along that pressure gradient, outwards or inwards as the case may be. Over and above these effects, there is the often observed phenomenon of "inwards pumping" that occurs in face seals. While inward pumping remains unexplained, Stanghan - Batch and Iny [2] suggest that the curvature of the seal faces produces a radial asymmetry in the pressure wave and induces a net inward flow of fluid across the faces. If the sealed fluid is placed on the inside of the sealing ring, this inward pumping effect can be utilized to suppress the flow of fluid across the faces due to the hydrostatic pressure gradient arising out of the centrifugal action of the sealed fluid pressure. However, this precise balance of flow is difficult to maintain in practice and should conditions change so that the inward pumping action exceeds the sealed fluid pressure, all fluid would be pumped out of the clearance between the faces, with disastrous consequences. Seals should therefore be designed to leak slightly to ensure that a lubricating film is maintained between the faces. The choice of an inside or outside seal configuration should also be made to suit the duty required of the seal. For moderate to high sealed fluid pressure, an inside seal should normally be used so that the inward pumping action can be utilized to limit the leakage. For

inside seals with low sealed fluid pressures, and particularly with high rotational speeds, the inward pumping action may be too great to be overcome by the hydrostatic fluid pressure at practical clearances. A more satisfactory design would result from arranging the sealed fluid on the outside of the seal ring, in which case a steady supply of fluid to the seal interface is assured although the leakage rate may be high.

In the present analysis an inside seal is chosen and the boundary conditions are  $p = p_s$  at  $r = r_i$  and  $p = 0$  at  $r = r_o$ . As equation (1.9) is much too cumbersome, further development of the pressure equation is postponed till after the development of an approximated equation for hydrodynamic pressure.

### 1.5 Squeeze Effect

From equation (1.5), the pressure distribution for only the squeeze effect is given by

$$\frac{1}{r} \frac{\partial}{\partial r} (h^3 r \frac{\partial p}{\partial r}) = 12 \mu (\bar{h} + \dot{\gamma} r \cos\theta) \quad (1.10)$$

$$\text{ie } \frac{\partial}{\partial r} (h^3 r \frac{\partial p}{\partial r}) = 12 \mu \bar{h} r + 12 \mu \dot{\gamma} r^2 \cos\theta$$

Integrating with respect to 'r'

$$h^3 r \frac{\partial p}{\partial r} = 12\mu \bar{h} \frac{r^2}{2} + 12\mu \dot{\gamma} \cos\theta \frac{r^3}{3} + C_s$$

$$\text{ie } \frac{\partial p}{\partial r} = \frac{6\mu \bar{h}r}{h^3} + \frac{4\mu \gamma \cos\theta r^2}{h^3} + \frac{C_s}{h^3 r}$$

Substituting for  $h$  from equation (2)

$$\frac{\partial p}{\partial r} = \frac{6\mu \bar{h}r}{(h + \gamma r \cos\theta)^3} + \frac{4\mu \gamma \cos\theta r^2}{(h + \gamma r \cos\theta)^3} + \frac{C_s}{(h + \gamma r \cos\theta)^3 r}$$

$$\text{ie } \frac{\partial p}{\partial r} = \frac{6\mu \bar{h}}{h^3} \frac{r}{(1 + \frac{\gamma r \cos\theta}{\bar{h}})^3} + \frac{4\mu \gamma \cos\theta}{h^3} \frac{r^2}{(1 + \frac{\gamma r \cos\theta}{\bar{h}})^3} + \frac{C_s}{h^3 r (1 + \frac{\gamma r \cos\theta}{\bar{h}})^3}$$

Integrating with respect to 'r' using tables of integration [3]

$$p = \frac{6\mu \bar{h}}{h^3} \frac{\bar{h}^2}{\gamma^2 \cos^2\theta} \left[ -\frac{1}{1 + \frac{\gamma \cos\theta r}{\bar{h}}} + \frac{1}{2(1 + \frac{\gamma \cos\theta r}{\bar{h}})^2} \right] \\ + \frac{4\mu \gamma \cos\theta}{h^3} \frac{\bar{h}^3}{\gamma^3 \cos^3\theta} \left[ \ln \left( 1 + \frac{\gamma \cos\theta r}{\bar{h}} \right) + \frac{2}{1 + \frac{\gamma \cos\theta r}{\bar{h}}} - \frac{1}{2(1 + \frac{\gamma \cos\theta r}{\bar{h}})^2} \right] \\ + \frac{C_s}{h^3} \left[ \frac{1}{2} \left( \frac{2 + \gamma \cos\theta r / \bar{h}}{1 + \gamma \cos\theta r / \bar{h}} \right)^2 + \ln \left( \frac{r\bar{h}}{1 + \gamma \cos\theta r / \bar{h}} \right) \right] + C_4 \quad (1.11)$$

Where  $C_s$  and  $C_4$  are constants of integration.

## 1.6 Approximation

Both equations (1.9) and (1.11) are much too cumbersome and an approximation, neglecting the radial variation of film thickness, is considered and the pressure distributions so derived are compared with the results from eqs, (1.9) and (1.11).

Thus film thickness is now given by,

$$h = \bar{h} + \gamma r_m \cos\theta \quad (1.12)$$

$$\frac{\partial h}{\partial \theta} = -\gamma r_m \sin\theta \quad (1.13)$$

$$\text{and } \frac{\partial h}{\partial t} = \bar{h} + \gamma r_m \cos\theta \quad (1.14)$$

Substituting in the Reynolds equation (1.1), with  $r = r_m$

$$\frac{\partial}{\partial r} \left( h \frac{\partial p}{\partial r} \right) = -6\mu\omega \gamma_m \sin\theta + 12\mu \bar{h} + 12\mu \gamma r_m \cos\theta$$

$$\frac{\partial}{\partial r} \left( h \frac{\partial p}{\partial r} \right) = -6\mu\gamma r_m \sin\theta\omega + 12\mu(\bar{h} + \gamma r_m \cos\theta) \quad (1.15)$$

## 1.7 Hydrodynamic Effect with Approximation

From equation (1.15), the pressure distribution for only the hydrodynamic effect is given by

$$\frac{\partial}{\partial r} \left( h^{\frac{3}{2}} \frac{\partial p}{\partial r} \right) = -6\mu\gamma r_m \sin\theta \omega \quad (1.16)$$

Integrating with respect to 'r'

$$h^{\frac{3}{2}} \frac{\partial p}{\partial r} = -6\mu\gamma r_m \sin\theta \omega r + C_1$$

Integrating again with respect to 'r'

$$p = \frac{-6\mu\gamma r_m}{h^{\frac{3}{2}}} \sin\theta \frac{\omega r^2}{2} + \frac{C_1 r}{h^{\frac{3}{2}}} + C_2$$

Where  $C_1$  and  $C_2$  are constants of integration

$$\text{i.e. } p = -\frac{3\mu\gamma}{h^{\frac{3}{2}}} r_m \sin\theta \omega r^2 + \frac{C_1 r}{h^{\frac{3}{2}}} + C_2 \quad (1.17)$$

With boundary conditions  $p = p_s$  at  $r_i$  and  $p = 0$  at  $r_o$

$$p_s = -\frac{3\mu\gamma}{h^{\frac{3}{2}}} r_m \sin\theta \omega r_i^2 + \frac{C_1 r_i}{h^{\frac{3}{2}}} + C_2 \quad (1.18)$$

$$\text{and } 0 = -\frac{3\mu\gamma}{h^{\frac{3}{2}}} r_m \sin\theta \omega r_o^2 + \frac{C_1 r_o}{h^{\frac{3}{2}}} + C_2 \quad (1.19)$$

Substracting (1.18) from (1.19)

$$-p_s = \frac{-3\mu\gamma}{h^{\frac{3}{2}}} r_m \sin\theta \omega (r_o^2 - r_i^2) + \frac{C_1}{h^{\frac{3}{2}}} (r_o - r_i)$$

$$\text{i.e. } C_1 = +\frac{h^{\frac{3}{2}}}{(r_o - r_i)} \left[ \frac{3\mu\gamma}{h^{\frac{3}{2}}} r_m \sin\theta \omega (r_o^2 - r_i^2) - p_s \right] \quad (1.20)$$

$$\text{and } C_2 = - \frac{r_o}{h^3} \left[ - \frac{p_s h^3}{(r_o - r_i)} + 3\mu\gamma r_m \sin\theta \omega (r_i + r_o) \right]$$

$$+ \frac{3\mu\gamma}{h^3} r_m \sin\theta \omega r_o^2$$

$$\text{ie } C_2 = - \frac{3\mu\gamma}{h^3} r_m \sin\theta \omega r_o r_i + p_s \frac{r_o}{(r_o - r_i)} \quad (1.21)$$

Substituting for  $C_1$  and  $C_2$  in (1.17)

$$p = \frac{3\mu\gamma}{h^3} r_m \sin\theta \omega r^2 + \frac{r}{h^3} 3\mu\gamma r_m \sin\theta \omega (r_i + r_o)$$

$$- \frac{3\mu\gamma}{h^3} r_m \sin\theta \omega r_i r_o + p_s \frac{(r_o - r)}{(r_o - r_i)}$$

$$\text{ie } p_h = \frac{-3\mu\gamma r_m \sin\theta \omega}{(\bar{h} + \gamma r_m \cos\theta)^3} \left[ r^2 - (r_o + r_i)r + r_o r_i \right] + p_s \frac{(r_o - r)}{(r_o - r_i)} \quad (1.22)$$

### 1.8 Squeeze Effect with Approximation

From equation (1.15), the pressure distribution for only the squeeze effect is given by

$$\frac{\partial}{\partial r} \left( h^3 \frac{\partial p}{\partial r} \right) = 12\mu (\bar{h} + \gamma r_m \cos\theta) \quad (1.23)$$

Integrating twice with respect to 'r'

$$p = \frac{6\mu}{h^3} (\bar{h} + \dot{\gamma} r_m \cos\theta) r^2 + \frac{C_3 r}{h^3} + C_4 \quad (1.24)$$

where  $C_3$  and  $C_4$  are constants of integration.

For boundary conditions,  $p = 0$  at  $r = r_i$  and  $p = 0$  at  $r = r_o$   
 (The condition  $p = p_s$  at  $r = r_i$  has already been incorporated in  
 the hydrodynamic pressure)

$$0 = \frac{6\mu}{h^3} (\bar{h} + \dot{\gamma} r_m \cos\theta) r_i^2 + \frac{C_3 r_i}{h^3} + C_4 \quad (1.25)$$

and

$$0 = \frac{6\mu}{h^3} (\bar{h} + \dot{\gamma} r_m \cos\theta) r_o^2 + \frac{C_3 r_o}{h^3} + C_4 \quad (1.26)$$

Subtracting (1.25) from (1.26)

$$0 = \frac{6\mu}{h^3} (\bar{h} + \dot{\gamma} r_m \cos\theta) (r_o^2 - r_i^2) + \frac{C_3}{h^3} (r_o - r_i)$$

$$\text{i.e. } C_3 = -6\mu (\bar{h} + \dot{\gamma} r_m \cos\theta) (r_o + r_i) \quad (1.27)$$

and

$$C_4 = \frac{6\mu}{h^3} (\bar{h} + r_m \cos\theta) (r_o r_i) \quad (1.28)$$

Substituting for  $C_3$  and  $C_4$  in equation (1.24)

$$P_{sq} = \frac{6\mu(\bar{h} + r_m \cos\theta)}{\bar{h} + r_m \cos\theta} \left[ r^2 - (r_o + r_i) r + r_o r_i \right] \quad (1.29)$$

### 1.9 Comparison of Results from the Complete and Approximate Equations for Pressure

Numerical data used in the comparison are as below.

$$\mu = 0.1 \text{ Pa.s i.e. SAE 10 oil at } 35^\circ\text{C.}$$

$$r_o = 0.052\text{m}$$

$$r_i = 0.048\text{m}$$

$$\text{so that, } r_m = 0.05\text{m}$$

$$\bar{h} = 2.54 \times 10^{-3}\text{m}$$

$$\text{Since } \frac{r_m}{\bar{h}} \leq 0.1, \text{i.e. } r_{\max} = \frac{0.1 \times 2.54 \times 10^{-3}}{0.05} = 5.08 \times 10^{-5} \text{ radians}$$

$$\cong 5.0 \times 10^{-5} \text{ radians}$$

The shaft speed ' $\omega$ ' is 3000 rpm

$$\text{i.e. } \omega = 50 \text{ rev/s.}$$

The value of  $r$  is also chosen as equal to 50 c/s. (This is just a convenient choice;  $r$  does not have to be equal to  $\omega$ . )

It may be noted that in each cycle the total traverse of  $r$  is 4 times  $r_{\max}$  (and not  $2\pi$ ).

$$\dot{r} = 4 \times (r_{\max}) \times 50 \text{ rad/sec}$$

$$= 10^{-2} \text{ rad/s}$$

For the numerical comparison, we choose a tilt  $r$ , which is half the maximum tilt ( $r_{\max}$ ),

$$\begin{aligned}\text{i.e. } r &= \frac{r_{\max}}{2} \\ &= 2.5 \times 10^{-3} \text{ radians.}\end{aligned}$$

#### Summary of Values

$$\mu = 0.1 \text{ Pa.s}$$

$$\bar{h} = 2.5 \times 10^{-3} \text{ m}$$

$$r = 2.5 \times 10^{-3} \text{ radians}$$

$$r_o = 0.052 \text{ m}$$

$$r_i = 0.048 \text{ m}$$

$$r_m = 0.05 \text{ m}$$

$$\omega = 3000 \text{ rpm}$$

$$\dot{r} = 0.01 \text{ rad/sec}$$

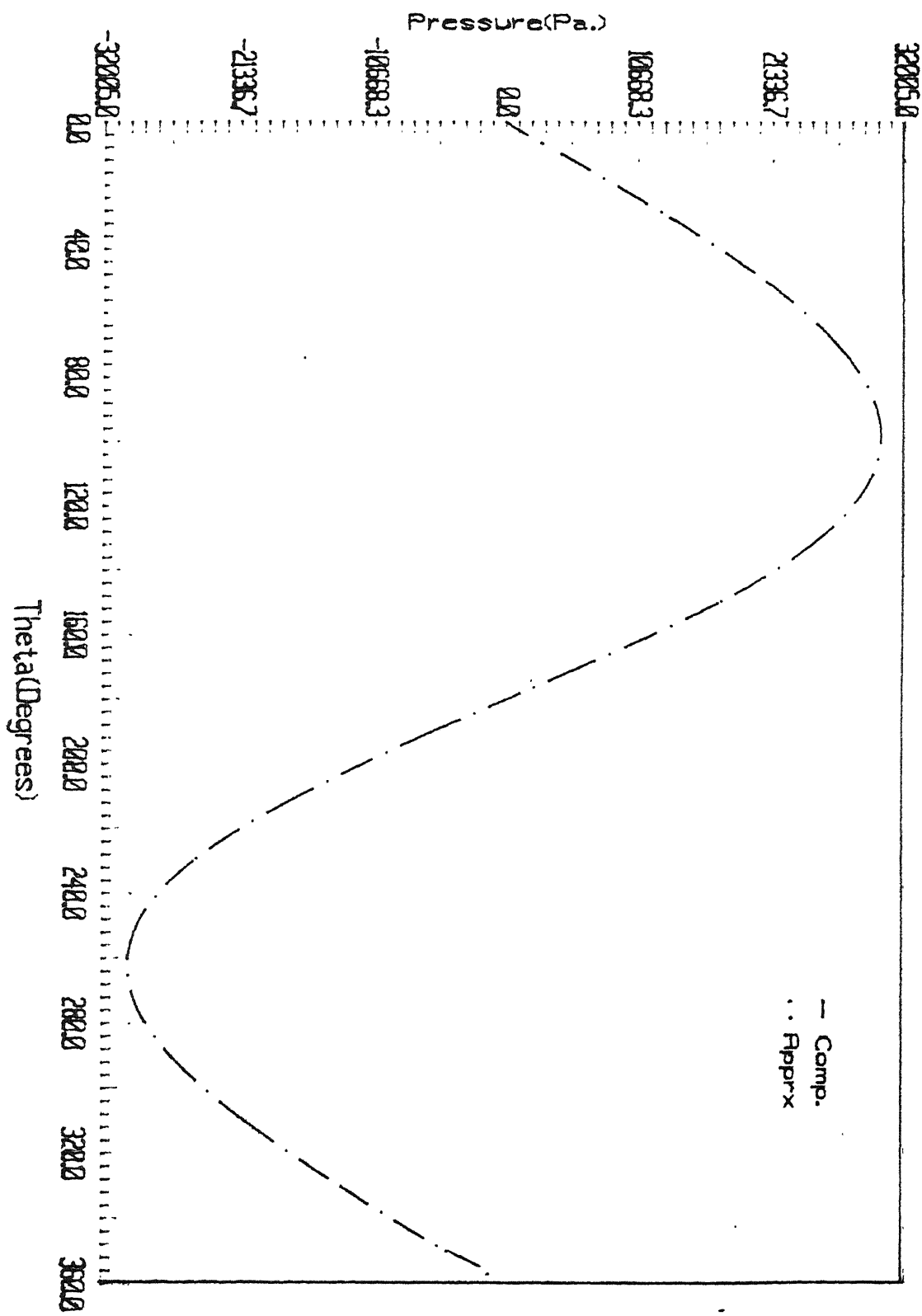


FIG. 1.5 HYDRODYNAMIC FILM PRESSURE COMPARISON

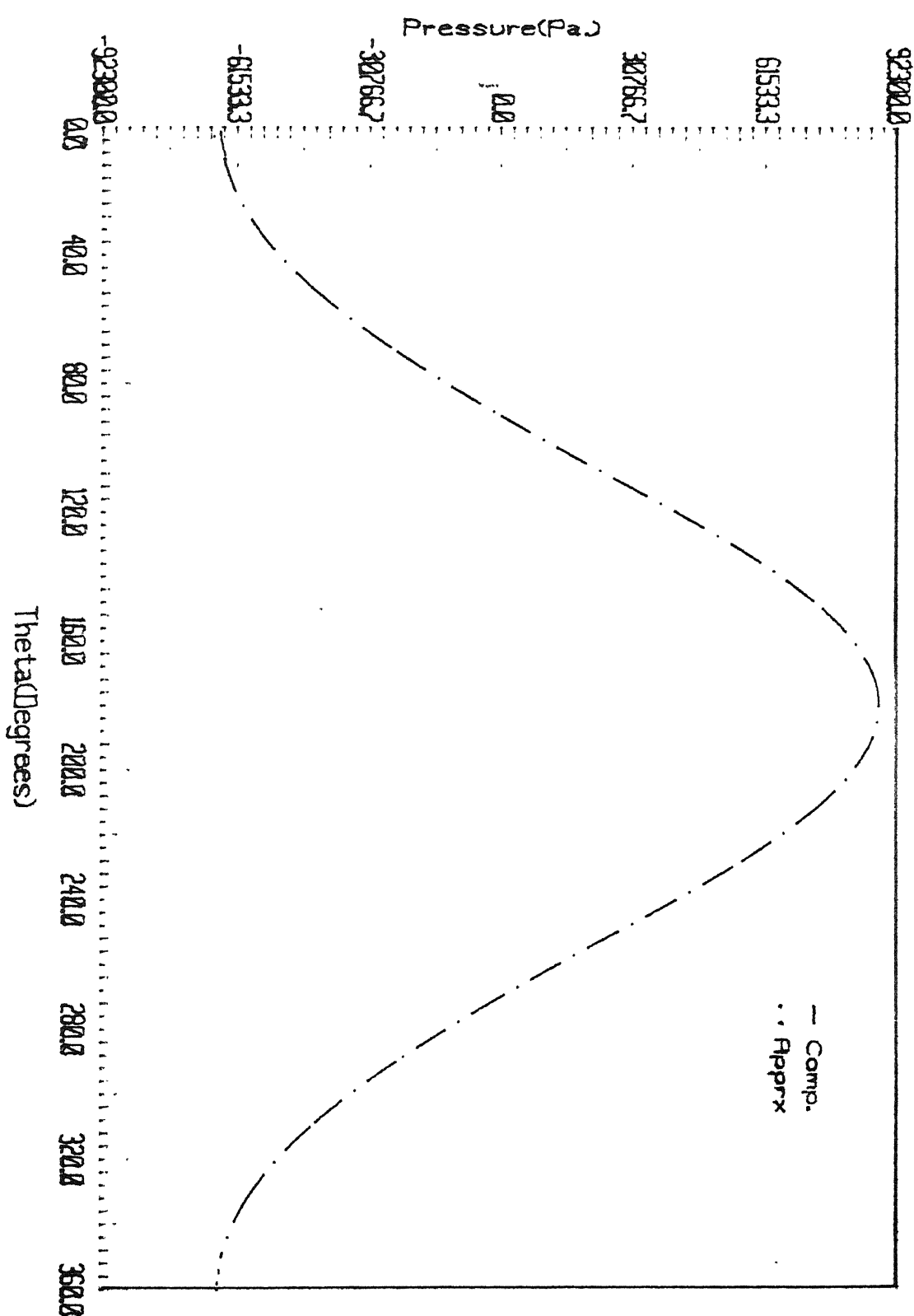


FIG. 1.6 SQUEEZE FILM PRESSURE COMPARISON

### **1.10 Results**

Fig. 1.5 shows the hydrodynamic film pressure distributions, using the complete and approximate equations i.e. equations (1.8) and

(1.22) respectively. Fig. 1.6, shows the squeeze film pressure distributions, using the complete and approximate equations ie equations (1.11) and (1.29) respectively. In both cases the error between the complete and approximate curves is below 2% ( the numbers are given in Appendix B) and hence not visible on the graph.

Thus comparison of the results from the complete and approximated equations show negligible differences in  $p(\theta)$ . One concludes that the variation of film thickness in the radial direction has a negligible effect on the overall circumferential film pressure distribution, and may be neglected.

### **1.11 Combined Effect of Film Forces**

Due to varying circumferential clearance in the seal interface, the fluid film has a converging and a diverging region. In the converging region, the viscous shear flow generated by the rotation forces the fluid into an ever - decreasing space, thus generating a positive pressure, which tends to force the seal rings apart against an external spring force. In the diverging region, a sub-atmospheric or negative pressure is developed. The negative

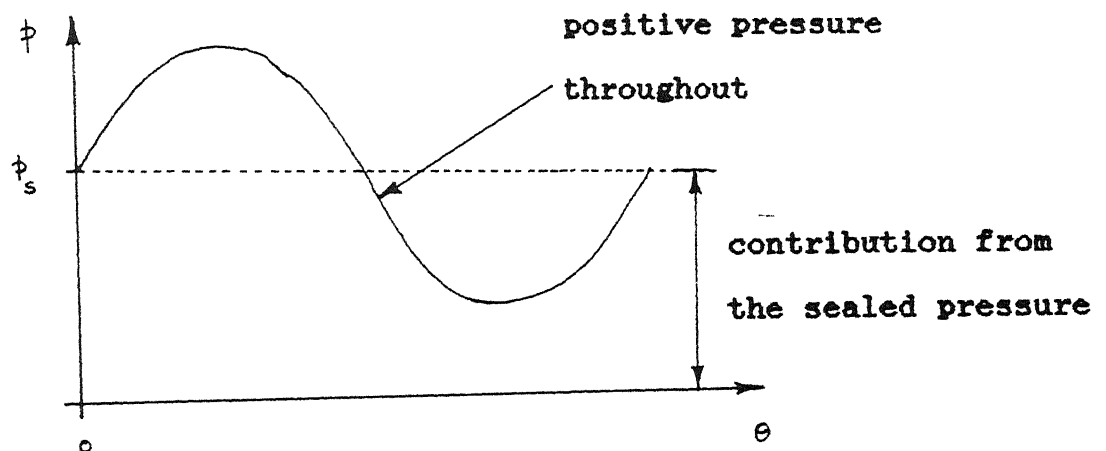
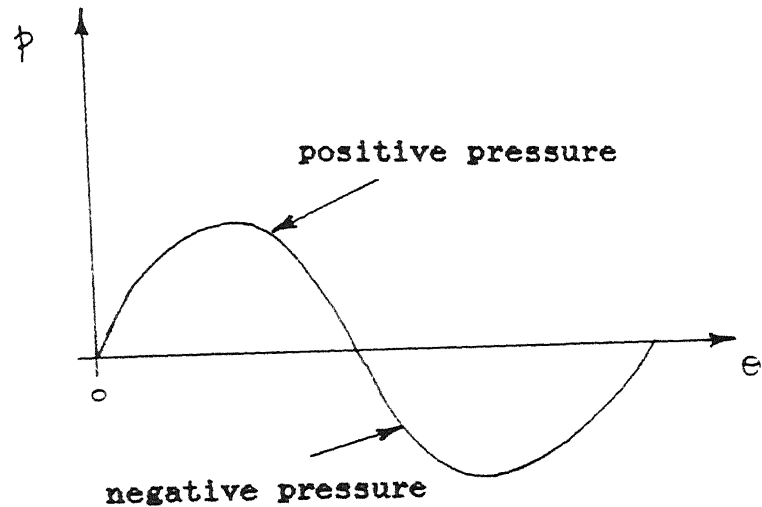


Fig. 1.7 Hydrodynamic film pressure distribution with and without large sealed pressure

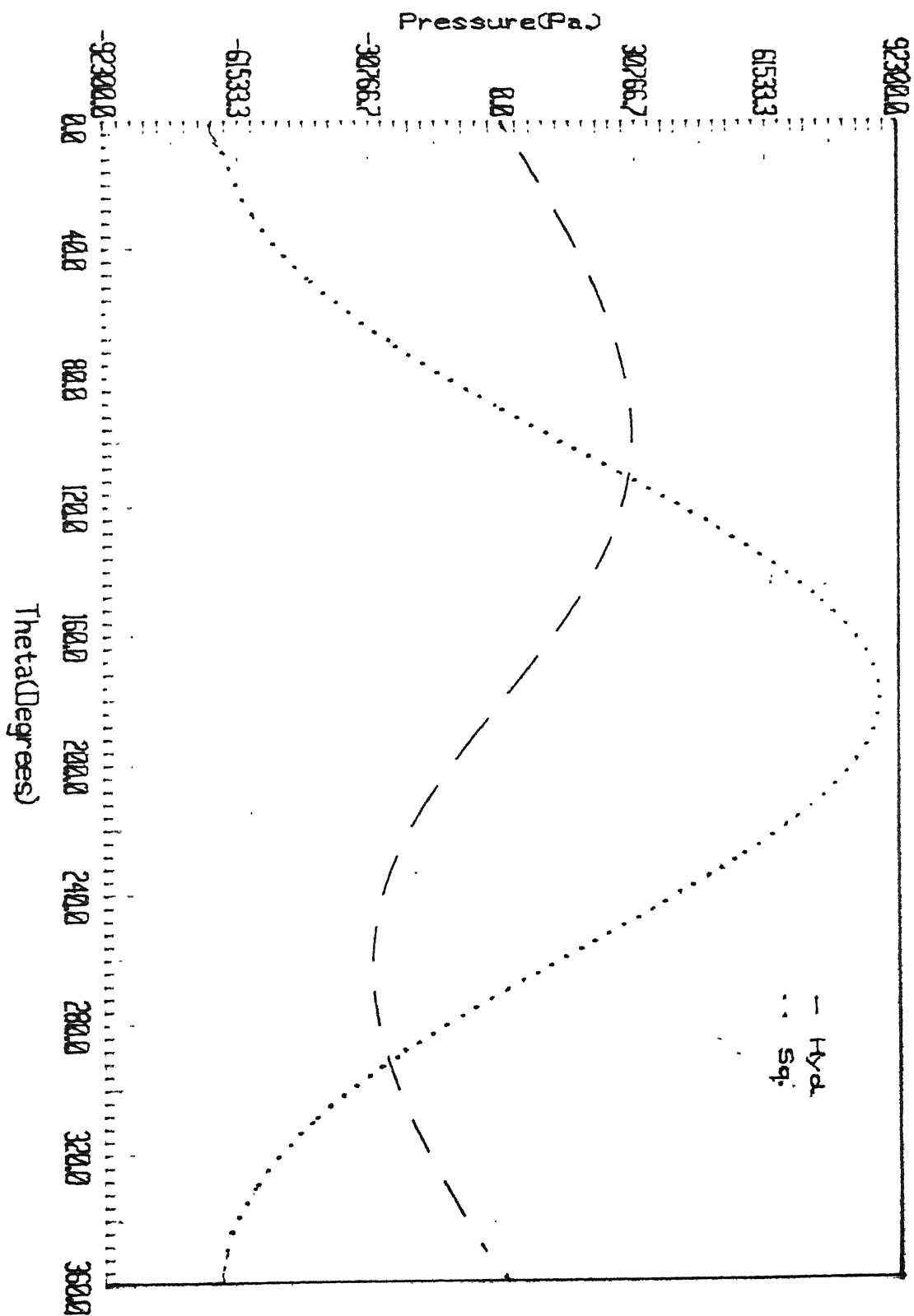
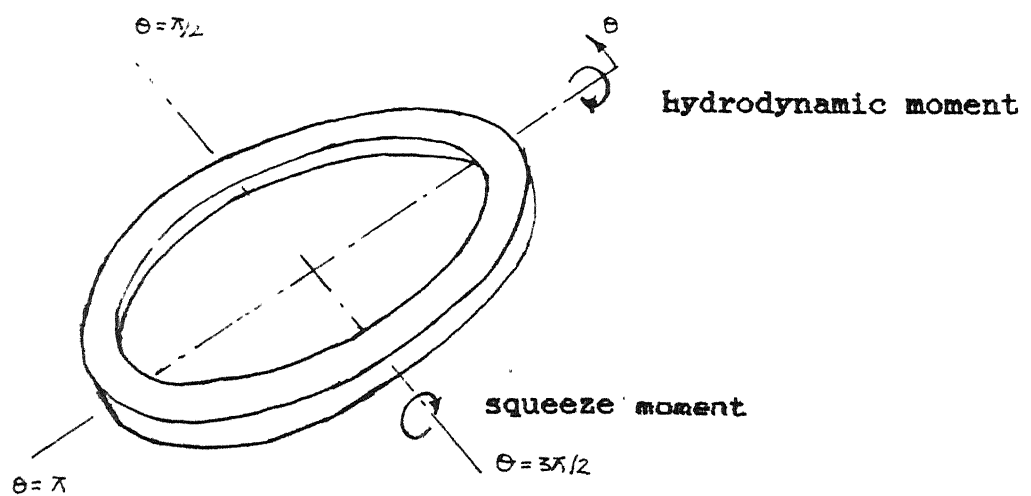


FIG. 1.8 FILM PRESSURE DISTRIBUTION



- Fig. 1.9 Hydrodynamic and squeeze moments on the stator ring.

pressure, if present, leads to localized cavitation in the form of vaporization of the fluid or release of dissolved gases from it. The sealed pressure is assumed to be sufficiently high to ensure that the net pressures do not fall below atmospheric, thereby avoiding cavitation.

Referring to figure 1.7, the constant part of the pressure, i.e. the sealed pressure  $p_s$ , contributes only to the axial force on the ring, and not to the moment. If  $p_s$  is sufficiently large,  $p$  can be positive everywhere and only the zero-average (i.e. sinusoidal) part of the net  $p$  contributes to the moment.

Figure(1.8) shows the circumferential variation of hydrodynamic and squeeze film pressures. The hydrodynamic film pressure is anti-symmetric about the axis defined by  $\theta = 0^\circ$  and  $180^\circ$  and therefore contributes to a moment purely about that axis (see figure 1.9). The squeeze film pressure is symmetric about the same axis and therefore contributes to a moment purely about a perpendicular axis. Thus the moments generated by hydrodynamic and squeeze action are about mutually perpendicular axes.

## Chapter 2

### 2.1 Dynamics of the Mechanical Face Seal

A schematic figure of the mechanical face seal model being analysed is shown in figure 1.3. The rotor-seat is rigidly mounted on the shaft with no axial translating freedom and perfect alignment. The stationary seal ring is flexibly mounted on bellows. Therefore the stator ring has an axial translation and two rotations about mutually perpendicular diameters. Both faces of the seal are flat, and the basis for generation of film pressures is the angular misalignment (tilt) of the stator ring.

The hydrodynamic and squeeze film pressure, and the spring forces, result in moments acting on the stator ring. The stator ring motion is analysed as a case of rigid body motion about its geometric centre. The geometric centre and mass centre of the stator ring are assumed to be coincident. Considering the two rotational degrees of freedom of the stator ring about mutually perpendicular axes, the body has two equations of motion.

### 2.2 The Co-ordinate system

In the derivation of the expressions for pressure no reference was made to a bi-axial tilt of either ring. Instead, it was simply assumed that a net inclination  $\gamma$  existed between the two rings and the film thickness was defined on that basis

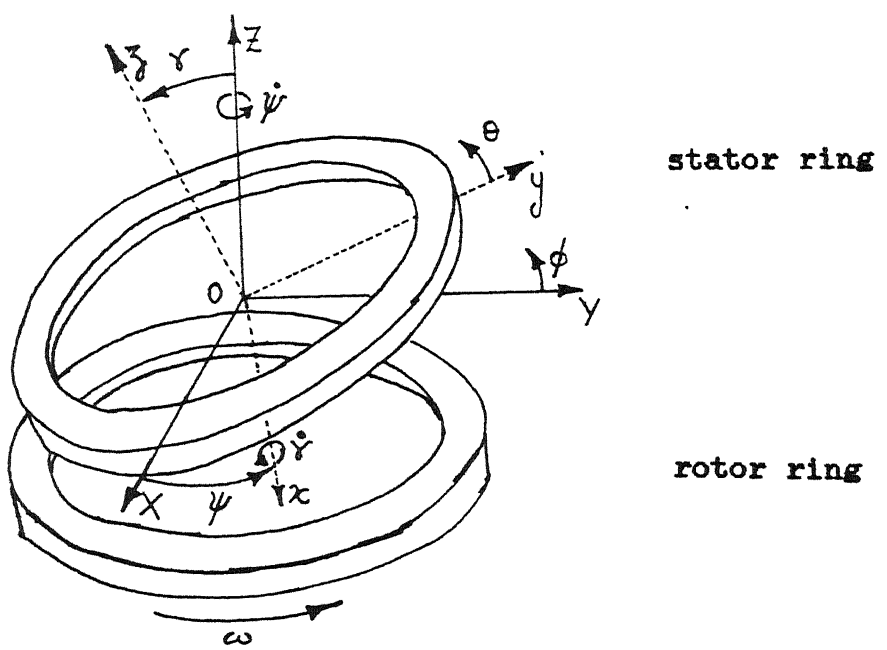


**Fig. 2.1** Coordinate system

[equation (1.12)]. If those results for pressure are to be directly usable, any subsequent choice of reference frame must preserve the conditions under which they were derived. Thus it is necessary to define a co-ordinate system in which the tilts can be described as about a single axis for all time. By definition, that axis must always be horizontal, i.e., parallel to the plane of the rotor ring.

The co-ordinate system used in subsequent derivations is shown in figure 2.1. The X,Y,Z axes comprise an inertial reference frame, fixed in space with the origin at the geometric centre 'O'. The X-O-Y plane is parallel to the rotating seat and the Z axis is the centre line of the shaft. The x,y,z axes constitute a rotating reference frame. The x-O-y plane is always in the plane of the stator ring. The angle of tilt  $\gamma$ , is the inclination of the axis of the stator ring relative to the vertical Z - axis and is also a measure of the angle between the planes containing the X,Y axes and the x,y axes. The angles  $\gamma$  and  $\psi$  are the Euler angles which specify the position of the x-y-z rotating reference frame with respect to the X-Y-Z inertial reference frame. The x-y-z rotating reference frame precesses about the Z-axis with angular velocity  $\psi$ , such that the x - axis always remains in the horizontal plane (i.e. in the X-O-Y plane), and the y-axis always passes through the point of maximum film thickness. Thus the x-y-z axes are the principal axes of the stator ring. The stator ring also nutates about the x-axis with angular velocity  $\dot{\gamma}$ .

### 2.3. Moment of Momentum Equations

The x-y-z axes and the stator ring have common nutation speeds about the x and y axes because the x-y plane is always in the plane of the stator. The x-y-z axes also have a spin about the z-axis which is not shared by the stator ring.

Referring to fig 2.1, the absolute angular velocity  $\vec{\omega}$  of the x-y-z axes in an inertial reference frame is seen to be

$$\vec{\omega} = \hat{i}\omega_x + \hat{j}\omega_y + \hat{k}\omega_z = \hat{i}\dot{\psi} + \hat{j}\dot{\psi} \sin\gamma + \hat{k}\dot{\psi} \cos\gamma \quad (2.1)$$

The components of velocity are thus  $\omega_x = \dot{r}$  (2.2)

$$\omega_y = \dot{\psi} \sin\gamma \quad (2.3)$$

$$\omega_z = \dot{\psi} \cos\gamma \quad (2.4)$$

The absolute velocity of the stator is

$$\vec{\alpha} = \hat{i}\Omega_x + \hat{j}\Omega_y + \hat{k}\Omega_z = \hat{i}\dot{\psi} + \hat{j}\dot{\psi} \sin\gamma$$

And the components of velocity are,  $\Omega_x = \dot{r}$  (2.5)

$$\Omega_y = \dot{\psi} \sin\gamma \quad (2.6)$$

$$\Omega_z = 0 \quad (2.7)$$

With principal axes of the present kind and different angular velocities for the body and the rotating x-y-z frame, the Euler equations are [4],

$$M_x = I_{xx} \dot{\Omega}_x - I_{yy} \Omega_y \omega_z + I_{zz} \Omega_z \omega_y \quad (2.8)$$

$$M_y = I_{yy} \dot{\Omega}_y - I_{zz} \Omega_z \omega_x + I_{xx} \Omega_x \omega_y \quad (2.9)$$

$$M_z = I_{zz} \dot{\Omega}_z - I_{xx} \Omega_x \omega_y + I_{yy} \Omega_y \omega_x \quad (2.10)$$

Since the stator ring is axisymmetric, we shall use the symbols

$$I_o = I_{xx} = I_{yy} \quad (2.11)$$

$$I = I_{zz} \quad (2.12)$$

Substituting for the components of velocity from equations (2.2) to (2.4) and (2.5) to (2.7) in the Euler equations,

$$M_x = I_o \frac{d}{dt} (\dot{r}) - I_o \dot{\psi}^2 \sin\psi \cos\psi \quad (2.13)$$

$$M_y = I_o \frac{d}{dt} (\dot{\psi} \sin\psi) + I_o \dot{r} \dot{\psi} \cos\psi \quad (2.14)$$

$$M_z = 0 \quad (2.15)$$

i.e.

$$M_x = I_o \ddot{r} - I_o \dot{\psi}^2 \sin\psi \cos\psi$$

$$M_y = 2I_o \dot{\psi} r \cos\gamma + I_o \ddot{\psi} \sin\gamma \quad (2.16)$$

For small  $\gamma$ , small tilts,

$$\sin\gamma \approx \gamma$$

$$\text{and } \cos\gamma \approx 1 \quad (2.17)$$

Using the relationships (2.17) in equations (2.16)

$$M_x = I_o \ddot{\gamma} - I_o \dot{\psi}^2 r \quad (2.18)$$

$$M_y = 2I_o \dot{\psi} \dot{\gamma} + I_o \ddot{\psi} r \quad (2.19)$$

These are the Euler equations for the stator ring.

The left hand sides of equations (2.18) & (2.19) represent moments acting on the stator ring. In this model, these moments, which are derived subsequently, are due to internal fluid film forces and the external spring force.

## 2.4 Fluid Film Generated Moments

### The Film thickness

Referring to figure 2.2, the varying circumferential clearance in the seal interface (i.e. the film thickness) when viewed from the inertial reference frame is a right running moving wave.

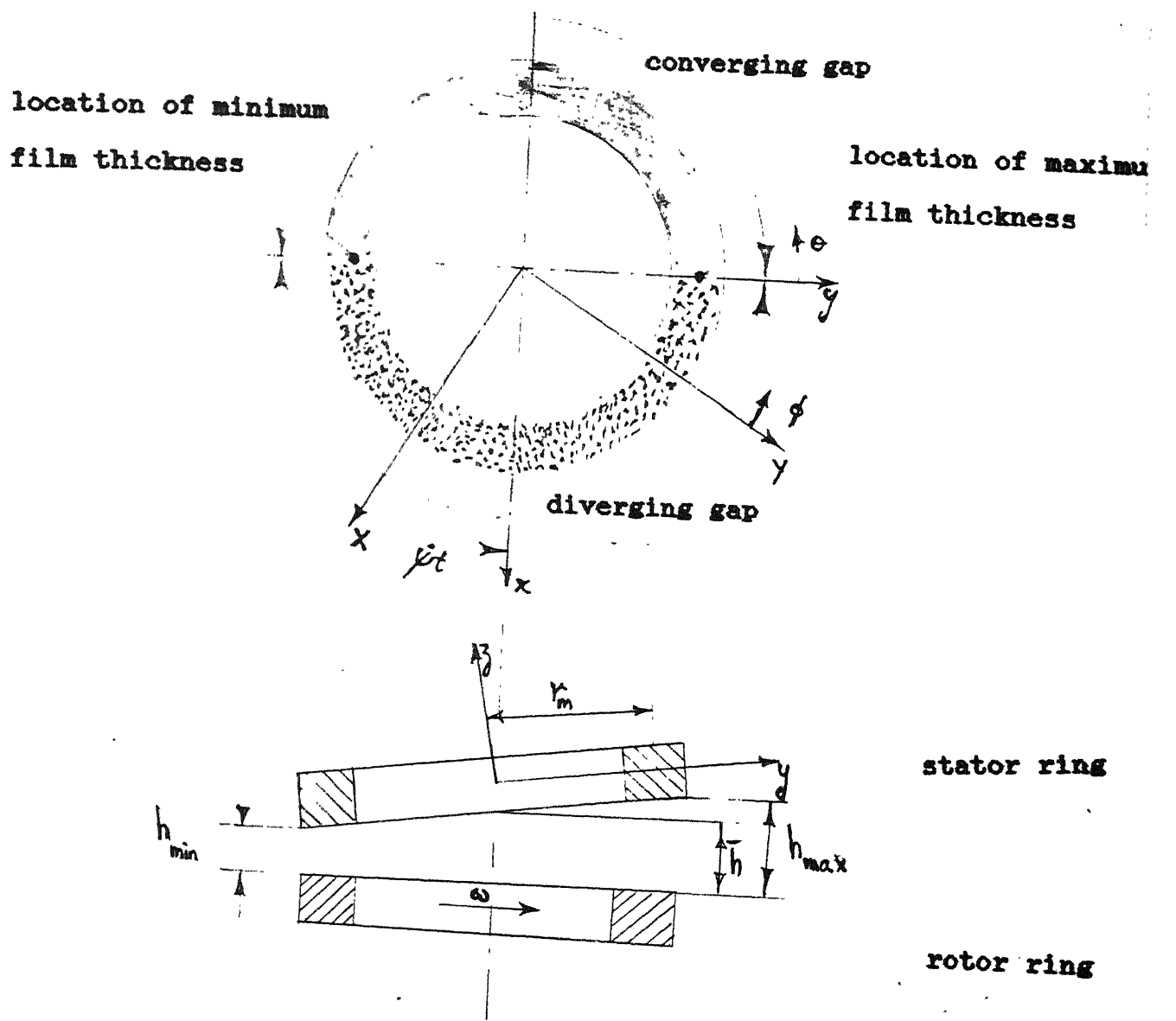


Fig. 2.2 Model for film thickness

Therefore,

$$h = \bar{h} + \gamma r_m \cos(\phi - \psi t) \quad (2.20)$$

$$\frac{\partial h}{\partial \phi} = -\gamma r_m \sin(\phi - \psi t) \quad (2.21)$$

$$\frac{\partial h}{\partial t} = \dot{\bar{h}} + \dot{\gamma} r_m \cos(\phi - \psi t) + \gamma r_m \dot{\psi} \sin(\phi - \psi t) \quad (2.22)$$

### The pressure equations

Substituting equations (2.21) and (2.22), in the Reynolds equation (1.1)

$$\begin{aligned} \frac{\partial}{\partial r} (h \frac{\partial p}{\partial r}) &= 6\mu \gamma r_m \sin(\phi - \psi t) (2\psi - \omega) + 12\mu (\bar{h} \\ &\quad + \dot{\gamma} r_m \cos(\phi - \psi t)) \end{aligned} \quad (2.23)$$

Using the same procedure as sections 1.7 and 1.8, the hydrodynamic and squeeze film pressure equations are given by,

$$p_{hyd} = \frac{3\mu r_m \sin(\phi - \psi t) (2\psi - \omega)}{[\bar{h} + \gamma r_m \cos(\phi - \psi t)]^3} [r^2 - (r_o + r_i)r + r_o r_i] + p_s \frac{(r_o - r)}{(r_o - r_i)} \quad (2.24)$$

$$p_{sq} = \frac{6\mu (\bar{h} + \dot{\gamma} r_m \cos(\phi - \psi t))}{[\bar{h} + \gamma r_m \cos(\phi - \psi t)]^3} [r^2 - (r_o + r_i)r + r_o r_i] \quad (2.25)$$

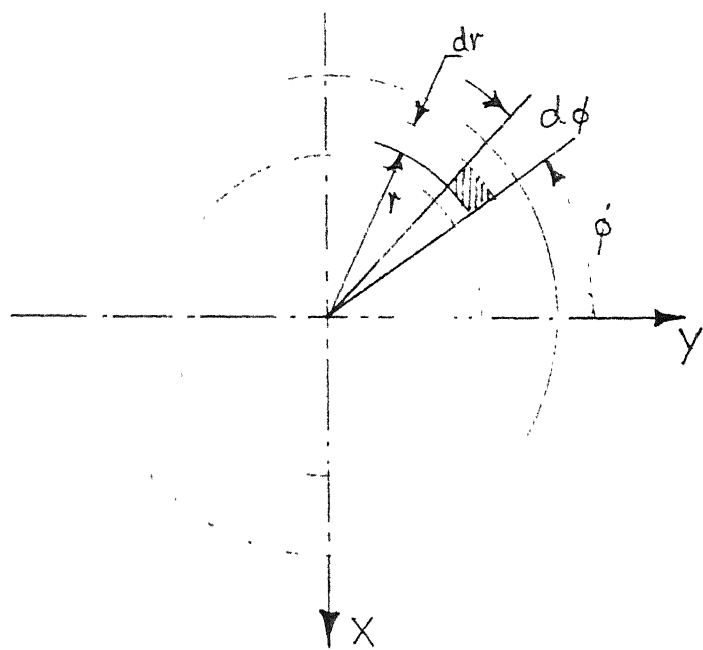


Fig. 2.3 Model for calculating moments

The moment equations

Referring to figure (2.3), the moment about the X axis due to the hydrodynamic film pressure is given by

$$(M_{hyd})_X = \int \int_{r \phi} r \cos\phi \left\{ p_{hyd} (rd\phi dr) \right\} \quad (2.26)$$

The limits of integration are  $r = r_i$  to  $r_o$  and  $\phi = 0$  to  $2\pi$ .

Substituting for  $p_{hyd}$  from equation (2.24) and noting that the sealed pressure term is constant throughout the circumference and therefore does not contribute to any moments,

$$(M_{hyd})_X = 3\mu\gamma r_m (2\dot{\gamma} - \omega) \int_{r_i}^{r_o} r^2 [r^2 - (r_o + r_i)r + r_o r_i] dr$$

$$\int_0^{2\pi} \frac{\cos\phi \sin(\phi - \dot{\gamma}t) d\phi}{[\bar{h} + \gamma r_m \cos(\phi - \dot{\gamma}t)]^3} \quad (2.27)$$

Referring to the appendix A and substituting the results (A1) (which defines a quantity R) and (A4) in equation (2.27)

$$(M_{hyd})_X = \frac{-3\mu\gamma r_m (2\dot{\gamma} - \omega) R \pi \sin \dot{\gamma}t}{\bar{h}^2} \quad (2.28)$$

Similarly, the moment about the Y axis, due to the hydrodynamic fluid film pressure is,

$$(M_{hyd})_Y = \int_{r_i}^{r_o} \int_0^{2\pi} r \sin\phi \{ p_{hyd} (rd\phi dr) \} \quad (2.29)$$

Substituting for  $p_{hyd}$  from equation (2.24), (2.24),

$$(M_{hyd})_Y = 3\mu\gamma r_m (2\dot{\psi} - \omega) \int_{r_i}^{r_o} r^2 [r^2 - (r_o + r_i)r + r_o r_i] dr$$

$$\int_0^{2\pi} \frac{\sin\phi \sin(\phi - \dot{\psi}t) d\phi}{[\bar{h} + \gamma r_m \cos(\phi - \dot{\psi}t)]^3} \quad (2.30)$$

Referring to the appendix A and substitution the results (A1) and (A5) in equation (2.30), we have

$$(M_{hyd})_Y = \frac{3\mu\gamma r_m (2\dot{\psi} - \omega) R \pi \cos\dot{\psi}t}{\bar{h}^3} \quad (2.31)$$

Similarly, the moment about the X axis due to the squeeze film pressure is

$$(M_{sq})_X = \int_{r_o}^{r_i} \int_0^{2\pi} r \cos\phi \{ p_{sq} (rd\phi dr) \} \quad (2.32)$$

The squeeze film pressure contains a term in  $\dot{h}$ . The quantity  $\dot{h}$  is the time rate of change of the mean film thickness  $\bar{h}$  and is non-zero when the seal closing force or external axial load varies with time. It may also be non-zero in the presence of transient film forces brought about by any perturbation in the geometry. The face load determines the equilibrium values of the mean film thickness, consistent with the amplitude of the film waviness. We shall assume here that the film profile represents an equilibrium configuration and that there is no externally induced vibration. Thus we may assume a constant  $\bar{h}$ , for which  $\dot{h} = 0$ . This assumption does weaken the model for the dynamics of the seal but is justified on the ground that the present analysis is a first attempt at understanding face seal dynamics and the inclusion of the extra unknown  $\dot{h}$  will introduce significant complexities in the model; for example,  $\dot{h}$  cannot be constant as that would imply a monotonic departure from any postulated  $\bar{h}$ . If  $\dot{h}$  is included in the analysis,  $\dot{h}$  must also be allowed for.

Substituting for  $p_{sq}$  from equation (2.25) and neglecting the contribution of  $\dot{h}$  to the squeeze - generated moments.

$$(M_{sq})_X = 6\mu r_m \int_{r_i}^{r_o} [r^2 - (r_o + r_i)r + r_o r_i] r^2 dr \int_0^{2\pi} \frac{\cos\phi \cos(\phi - vt)d\phi}{[\bar{h} + \gamma r_m \cos(\phi - vt)]^3}$$
(2.33)

Referring to the appendix A and substituting the results (A1) and (A6) in equation (2.33).

$$(M_{sq})_X = \frac{6\pi\mu r_m R \cos \psi}{h^3} \quad (2.34)$$

Similarly, the moment about the Y axis due to squeeze film pressure is

$$(M_{sq})_Y = \frac{6\pi\mu r_m R \sin \psi}{h^3} \quad (2.35)$$

The hydrodynamic moment which is purely about the y axis is given by the resultant of equations (2.28) and (2.31). Thus

$$(M_{hyd})_y = \frac{6\pi\mu r_m R (\psi - \omega/2)\gamma}{h^3} \quad (2.36)$$

Similarly, the squeeze moment, which is purely about the x axis, is given by the resultant of equations (2.34) and (2.35). Thus

$$(M_{sq})_x = \frac{6\pi\mu r_m R}{h^3} \quad (2.37)$$

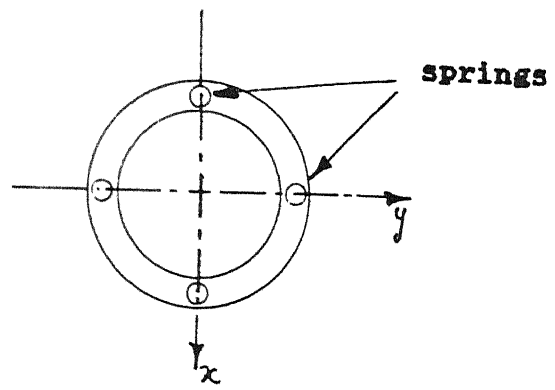


Fig. 2.4 Model for the Bellows

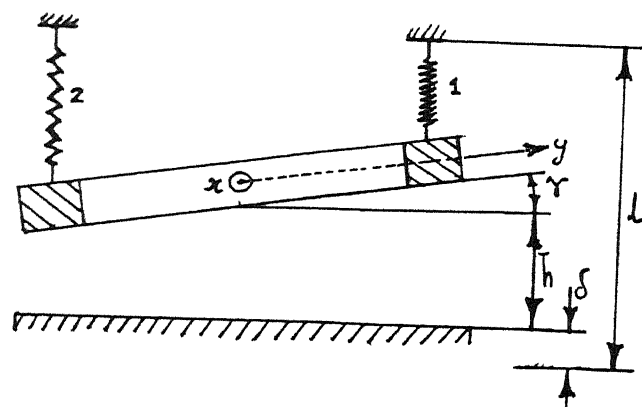


Fig. 2.5(a) Model for spring displacements

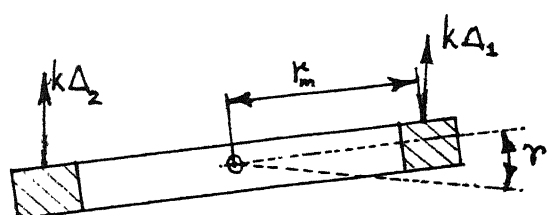


Fig. 2.5(b) Free body diagram of the stator ring  
showing spring forces

## 2.5 Moments Due to the Bellows

The support arrangement consisting of the bellows is modelled as equivalent of four equally spaced springs, each of stiffness 'k' acting at the mean radius  $r_m$ . The springs are assumed to lie on the x and y axes [fig. 2.4].

At any given tilt, which is always purely about the x axis, the spring force is distributed symmetrically about the y axis and therefore produces a moment purely about the x axis. Figure (2.5(a) shows the deflection of two springs on the positive y axis and negative y axis respectively, when the stator has tilted by an angle  $\gamma$  about the x-axis. The positive x axis is in a direction out of the plane of the paper.

Spring displacement is given by

$$\Delta = l - l_{\text{new}} \quad (2.38)$$

where,

$$l_{\text{new}} = l - \delta - h \quad (2.39)$$

$\delta$  = initial spring compression

Substituting for  $h$  from equation (2.20), in (2.39)

$$l_{\text{new}} = l - \delta - \bar{h} - \gamma r_m \cos(\phi - \dot{\psi}t) \quad (2.40)$$

On the positive y axis,  $\phi = \omega t$ , therefore

$$l_{\text{new}} = l - \delta - \bar{h} - \gamma r_m \quad (2.41)$$

Substituting equation (2.41) in (2.38), the spring displacement of spring '1' is,

$$\Delta_1 = \delta + \bar{h} - \gamma r_m \quad (2.42)$$

Similarly, on the negative y axis,  $\phi = \omega t + \pi$ , and the spring displacement of spring '2' is therefore,

$$\Delta_2 = \delta + \bar{h} + \gamma r_m \quad (2.43)$$

Taking moments about the x axis, (fig. 2.5 (b))

$$\left[ M_{sp} \right]_x = -k(\delta + \bar{h} + \gamma r_m) r_m \cos \gamma + k (\delta + \bar{h} - \gamma r_m) r_m \cos \gamma$$

$$\left[ M_{sp} \right]_x = -2kr_m^2 \gamma \cos \gamma \quad (2.44)$$

For small  $\gamma$ ,  $\cos \gamma \approx 1$ , thus,

$$\left[ M_{sp} \right]_x = -2kr_m^2 \gamma \quad (2.45)$$

$\left[ M_{sp} \right]_y$  is equal to zero.

## 2.6. The Equations of Motion

Substituting for the moments about the x and y axes given by equations (2.37), (2.45) and (2.36) respectively, in the equations of motion (2.18) and (2.19), the equations of motion are

$$\frac{6\pi\mu r_m R}{h^3} - 2kr_m^2 \dot{\gamma} = I_o \ddot{\gamma} - I_o \dot{\psi}^2 \gamma \quad (2.46)$$

$$\text{and } \frac{6\pi\mu r_m R}{h^3} - (\dot{\psi} - \omega/2)\gamma = 2I_o \dot{\psi} \dot{\gamma} + I_o \ddot{\psi} \gamma \quad (2.47)$$

$$\text{Let, } A = \frac{-6\pi\mu r_m R}{I_o h^3} = \frac{6\pi\mu r_m |R|}{I_o h^3} \quad (2.48)$$

$$\text{and } B = 2kr_m^2/I_o \quad (2.49)$$

thus, the equations of motion are,

$$\ddot{\gamma} + A \dot{\gamma} + (B - \dot{\psi}^2) \gamma = 0 \quad (2.50)$$

$$\text{and } \dot{\gamma} + \frac{A}{2} \left(1 - \frac{\omega}{2\dot{\psi}} - \dot{\psi}\gamma/2\dot{\psi}\right) \gamma = 0 \quad (2.51)$$

The equations (2.50) and (2.51), as they stand, have time dependent coefficients for  $\gamma$ . In fact if  $\dot{\psi}$  is a time dependent

quantity, the equations are non-linear and become intractable. The rotor however has a constant angular velocity  $\omega$ . The precision angular velocity of the rotating reference frame along the z axis, viz.  $\dot{\psi}$ , occurs in response to  $\omega$  and may be assumed to be constant when  $\omega$  is constant. Thus  $\dot{\psi}$  is assumed to be zero and equation (2.51) becomes,

$$\ddot{r} + \frac{A}{2} \left(1 - \frac{\omega}{2\dot{\psi}}\right)r = 0 \quad (2.52)$$

in which  $\dot{\psi}$  is constant.

Equation (2.50) is now a second-order, linear, ordinary differential equation in  $r$ , having constant coefficients. Its solution will be the solution for a damped spring-mass system; the damping term coefficient 'A' is positive because  $R$  is negative (eq. 2.48), and so the solution will correspond to the over damped, under-damped or critically damped case depending on the damping coefficient. Equation (2.52), on the other hand, is a first order, linear, ordinary differential equation which can have

a non-trivial solution of an exponential growth or decay. That is, equation (2.52) does not admit of an oscillatory solution.

The quantity  $\dot{\psi}$  represents a wobble of the stator ring. Although this quantity, has been assumed to be constant, it is an unknown and so it is appropriate to have the two equations (2.50) and (2.52) to describe the motion. It is necessary, however, for

these equations to give the same solution for  $\gamma$  for all time. It follows that, if eq. (2.52) does not have an oscillatory solution, neither can eq (2.50). A simultaneous solution to equations (2.50) and (2.52) is now sought.

Differentiating equation (2.52) with respect to time, we get,

$$\ddot{\gamma} + \frac{A}{2} \left(1 - \frac{\omega}{2\psi}\right) \dot{\gamma} = 0 \quad (2.53)$$

Comparing equation (2.50) with (2.53)

$$A\dot{\gamma} + (B - \dot{\psi}^2)\gamma = \frac{A}{2} \left(1 - \frac{\omega}{2\psi}\right) \dot{\gamma}$$

$$\text{i.e. } \frac{A}{2} \left(1 + \frac{\omega}{2\psi}\right) \dot{\gamma} + (B - \dot{\psi}^2)\gamma = 0 \quad (2.54)$$

Equation (2.54) has an exponential solutions. Therefore let

$$\gamma = \gamma_0 e^{\lambda t} \quad (2.55)$$

$$\text{and } \dot{\gamma} = \lambda \gamma_0 e^{\lambda t} \quad (2.56)$$

Substituting for  $\gamma$  and  $\dot{\gamma}$  from equations (2.55) and (2.56) respectively, in equation (2.54) we get

$$\lambda = -\frac{2}{A} \left[ \frac{(B-\dot{\psi}^2)}{1 + \frac{\omega}{2\dot{\psi}}} \right] \quad (2.57)$$

Substituting for  $\lambda$  from equations (2.57) in (2.55), the exponential solutions is

$$r = r_0 e^{\frac{-2}{A} \left[ \frac{(B-\dot{\psi}^2)}{1 + \frac{\omega}{2\dot{\psi}}} \right] t} \quad (2.58)$$

Three cases now present themselves, depending upon the relative sizes of  $\dot{\psi}^2$  and  $B$ .

CASE 1. If  $\dot{\psi}^2 > B$ ,  $r$  grows exponentially.

CASE 2. If  $\dot{\psi}^2 < B$ ,  $r$  decays exponentially.

CASE 3. If  $\dot{\psi}^2 = B$ ,  $r = r_0$ , i.e.  $r$  does not change.

The 'CASE 3' is of principal interest. Using the definition of  $B$  (e.g. 2.49), it says that the face inclination remains constant if,

$$\dot{\psi}^2 = 2kr_m^2/I_0 \quad \text{CENTRAL LIBRARY} \quad (2.59)$$

$$\text{i.e. } \dot{\psi} = r_m \sqrt{\frac{2k}{I_0}} \quad \text{Acc. No. } 113089 \quad (2.60)$$

Equation (2.60) shows that the wobble frequency increases with increasing mounting stiffness and decreases with increasing transverse moment of inertia of the stator ring. This is as it should be. A "softer" support or a greater inertia will both make the stator ring more sluggish and its response frequency will be less. Conversely, if the stator ring has zero inertia, it will respond to the slightest impetus and will not sustain any moment.

From equation (2.52), the corresponding condition for constant  $\gamma$  is

$$1 - \frac{\omega}{2\dot{\psi}} = 0$$

i.e.  $\dot{\psi} = \omega/2$  (2.61)

Substituting for  $\dot{\psi}$  from equation (2.61) in equation (2.60)

$$\omega = \sqrt{\frac{8kr_m^2}{I_0}}$$
 (2.62)

We now look for conditions which give other possible solutions to equations (2.50) and (2.52).

Equation (2.50) also has an exponential solution.

Therefore using the same definition of  $\gamma$  as in equation (2.55) the characteristic equation for (2.50) is

$$\lambda_{II}^2 + A\lambda_{II} + (B - \dot{\psi}^2) = 0 \quad (2.63)$$

where the subscript II refers to the second order equation (2.50)

$$\text{i.e. } \lambda_{II} = \frac{-A \pm \sqrt{A^2 - 4(B - \dot{\psi}^2)}}{2} \quad (2.64)$$

Equations (2.64) indicates the conditions for real  $\lambda_{II}$  (it must be real to simultaneously satisfy eq. (2.52)) is,

$$A^2 \geq 4(B - \dot{\psi}^2) \quad (2.65)$$

Just as the 'CASE 1' above indicate that for  $\dot{\psi}^2 > B$ ,  $\gamma$  grows exponentially, so also does equation (2.64) indicate a growing  $\gamma$  for the same condition.

Using the definitions for A and B from equations (2.48) and (2.49) respectively,

$$\left( \frac{6\pi\mu r_m |R|}{I_o h^2} \right)^2 \geq 4 \left( \frac{2kr_m^2}{I_o} - \dot{\psi}^2 \right) \quad (2.66)$$

$$\text{i.e. } \dot{\psi}^2 \geq r_m^2 \left[ \frac{2k}{I_0} - \left( \frac{3\pi\mu}{2I_0 h^2} \right)^2 R^2 \right] \quad (2.67)$$

Equation (2.67) sets a minimum value on  $\dot{\psi}$  for real  $\lambda_{II}$ .

Similarly, equation (2.52) also has an exponential solution and the characteristic equation is,

$$\lambda_I + \frac{A}{2} \left( 1 - \frac{\omega}{2\dot{\psi}} \right) = 0$$

$$\text{i.e. } \lambda_I = -\frac{A}{2} (1 - \omega/2\dot{\psi}) \quad (2.68)$$

For both equation (2.50) and (2.52) to have a common solution,  $\lambda_I$  and  $\lambda_{II}$  must be equal. Thus from equations (2.68) and (2.64).

$$-\frac{A}{2} (1 - \omega/2\dot{\psi}) = -\frac{A}{2} \pm \frac{1}{2} \sqrt{A^2 - 4(B - \dot{\psi}^2)} \quad (2.69)$$

Simplifying and rearranging terms we get,

$$\dot{\psi}^4 + (\frac{A^2}{4} - B)\dot{\psi}^2 - (\frac{A\omega}{4})^2 = 0 \quad (2.70)$$

The four roots of the quartic equation (2.70) are, (appendix C)

$$\dot{\psi}_{1,2} = \frac{1}{2} \sqrt{B - \frac{A^2}{4} + \frac{A\omega}{2}} \pm \frac{1}{2} \sqrt{B - \frac{A^2}{4} - \frac{A\omega}{2}}$$

$$\text{and, } \dot{\psi}_{3,4} = \frac{-1}{2} \sqrt{B - \frac{A^2}{4} + \frac{A\omega}{2}} \pm \frac{1}{2} \sqrt{B - \frac{A^2}{4} - \frac{A\omega}{2}} \quad (2.71)$$

From equation (2.71), the condition for which  $\dot{\psi}$  is real is,

$$B \geq \frac{A^2}{4} + \frac{A\omega}{2} \quad (2.72)$$

$$\text{i.e. } B \geq \frac{A}{2} \left( \frac{A}{2} + \omega \right) \quad (2.73)$$

Using the definitions for A and B given by equations (2.48) and (2.49) respectively,

$$\frac{2kr_m^2}{I_o} \geq \frac{6\pi\mu r_m |R|}{I_o \bar{h}^2} \left\{ \frac{6\pi\mu r_m |R|}{I_o \bar{h}^2} + \omega \right\} \quad (2.74)$$

Simplifying and rearranging terms,

$$\frac{2k r_m^2}{3\pi\mu |R| r_m} [\bar{h}^2]^2 - \omega \bar{h}^2 - \frac{3\pi\mu r_m |R|}{I_o} \geq 0 \quad (2.75)$$

Equation (2.75) sets a condition on  $\bar{h}^2$ , namely that the minimum  $\bar{h}^2$  is,

$$\bar{h}^2 = \frac{3\pi\mu |R|}{4kr_m} \left[ \omega \pm \sqrt{\omega^2 + \frac{8kr_m^2}{I_o}} \right] \quad (2.76)$$

Substituting for the half frequency solution i.e. equation (2.62) in equation (2.76),

$$\bar{h}^2 = \left[ \frac{3\pi\mu|R|}{4kr_m} \right] \left[ \omega (1 \pm \sqrt{\frac{1}{2}}) \right] \quad (2.77)$$

As  $\bar{h}$  is a positive quantity, the only acceptable condition for  $\bar{h}^2$  is,

$$\bar{h}^2 = \left[ \frac{3\pi\mu|R|}{4kr_m} \right] \left[ \omega (1 + \sqrt{\frac{1}{2}}) \right]$$

Using eq. (2.62) again for the half-frequency wobble condition, the above expression becomes

$$\bar{h}^2 = \frac{6\pi\mu r_m |R|}{I_o} \frac{1 + \sqrt{\frac{1}{2}}}{\omega} \quad (2.78)$$

## CHAPTER 3

### 3.1. Main Results

It is found that, with a small angular misalignment between the seal faces, the radial variation in the film thickness can be neglected because it has almost no effect on the hydrodynamic and squeeze film pressure. Consequently, it also has negligible effect on the fluid film-generated moments and thus on the face seal dynamics.

For the analysis of the face seal dynamics, the mean film thickness is assumed to be constant. It is postulated that the stator ring wobbles in response to the rotation of the rotor and that, the shaft angular speed being nominally constant, the stator has a steady wobble frequency. The stator is flexibly mounted and is modelled as a flat but tilted ring. The wobble is modelled as a rotation of the stator tilt axis about the shaft centre line.

With the above assumptions, two equations of motion are obtained for two mutually perpendicular components of the net tilt. It is found that these equations give only one meaningful solution, that of a steady-state wobble with constant amplitude as well as frequency. The corresponding wobble frequency is one-half of the shaft or rotating ring frequency. This finding would appear to corroborate the experimental observation of Burton and Etsion [5]. Working with a set-up that duplicates the present

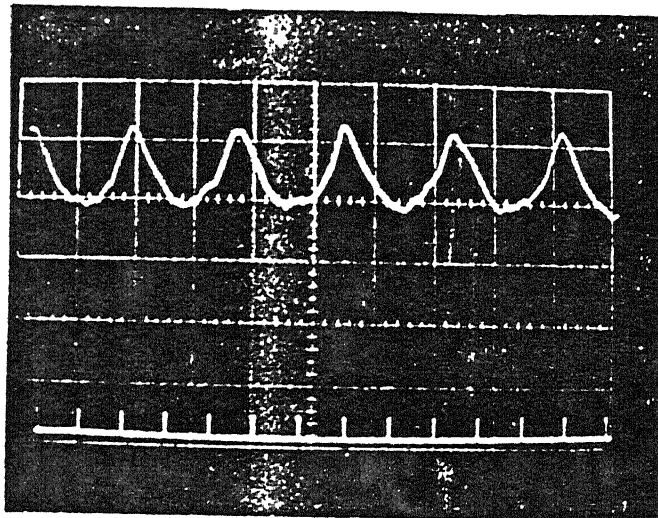


Fig. 3.1 Signals showing a wobble frequency approximately  
half the frequency of rotation [5]

theoretical model, they found a steady operating condition in which the flexibly mounted stator ring wobbled at a frequency close to half the shaft speed. Their result is reproduced here in fig. (3.1), in which two oscilloscope traces are shown. The lower beam is a timing pulse, which serves to indicate the frequency of rotation of the rotor, whereas the upper beam indicates the wobble frequency. It may be readily seen that there are approximately half the number of pulses on the upper beam as on the lower beam.

Looking back at the expressions for pressure, it is seen that the steady state wobble, for which the amplitude  $\gamma$  is constant, leads to zero squeeze film pressure unless the mean film thickness  $\bar{h}$  varies with time (eq.1.29). This occurs because  $\dot{\gamma} = 0$ . Interestingly, the hydrodynamic pressure (eq. 1.22) also becomes zero because of the wobble frequency  $\dot{\psi}$  being one - half of the shaft speed  $\omega$ , except for the constant term in  $p_s$ , the sealed fluid pressure. This constant term provides some axial force against face closure if  $p_s$  is significant, but does not generate a moment. So the steady wobble solution leads to zero moment. The fluid film still exists but has no resilience. It also generates no pressure with which to seal the leakage. In other words, the hydrostatic pressure gradient across the seal face, due to the sealed fluid pressure, causes fluid to leak out and the seal to fail.

The constant  $\gamma$  or half-frequency wobble state is akin to a neutral state of equilibrium with no fluid film resilience. Any disturbance of this state will therefore be unresisted by film forces. An increased or decreased tilt will be accompanied by a small departure in the threshold value of  $\psi$  (eq. 2.60) and a shift to the exponential growth or decay solutions respectively. In the latter case, the stator tilt will be neutralised whereas in the former the stator and rotor rings will tend to come into physical contact. Either event will mean seal failure.

The situation is analogous to the half-frequency whirl in hydrodynamic journal bearings. In that case, the journal centre whirls at one-half of the shaft speed resulting in zero hydrodynamic pressure and zero load-support in the bearing. The half-frequency wobble of the seal face given by the present solution also results in zero fluid film pressure.

The condition for  $\bar{h}^*$  (eqn. 2.78) is a means of calculating the mean film thickness in order to estimate the leakage at the half frequency wobble condition.

Other dynamic states are no doubt possible. To obtain them, a fuller analysis will be required. For example, if the  $\dot{h}$  term is included in the analyses (i.e. if axial vibrations of the seal are allowed), that will give a non-zero squeeze - film moment. The extra equation required to solve for the extra unknown  $\dot{h}(t)$  will

be the second order differential equation in  $\bar{h}(t)$ , describing the axial translatory dynamics of the seal ring. Based on the present experience, it can perhaps be anticipated that the said equation will also be non-linear. Of course, a complete dynamic analysis will have to accommodate a time-varying wobble  $\psi(t)$  but that, it is seen, will lead to strongly non-linear equations of motion. Finally, the hydrostatic pressure gradient may also generate transverse moments in the flexibly - mounted seal ring [6] and influence its dynamic behaviour.

The present half-frequency wobble solution requires two conditions to be satisfied simultaneously. These conditions are stated in eqs (2.60) and (2.62). Equation (2.62) is the necessary but not sufficient condition for eq. (2.61). In other words, the half frequency wobble does not necessarily follow if eq. (2.62) is satisfied. Thus it is suggested that the design of the seal should be done with an eye on conditions (2.62) and  $k$  and  $I_o$  so chosen that, for the shaft speed dictated by the particular application, condition (2.62) is not fulfilled. Specifically, in order to avoid a case of exponential growth of  $\gamma$  or a case of constant  $\gamma$ , the condition,

$$\omega < \sqrt{\frac{8kr^2}{I_o}}$$

must be satisfied. Thus  $k$  and  $I_o$  must be so chosen for the shaft speed dictated by the particular application.

## CONCLUSION

The flexibly mounted stator ring has two degrees of freedom. Its motion, in response to the rotation of the rotor ring consists of a wobble and is described by two non-linear differential equations for two mutually perpendicular components of the net tilt of the stator. The equations are reduced to linear form by assuming constant wobble frequency and conditions are found for the tilt to increase, decrease or remain constant. It is found that when the condition for constant tilt is satisfied the wobble frequency of the stator ring is one-half of the shaft or rotating ring frequency. This state results in zero fluid film moments, causing failure of the seal. Equation (2.62) gives a relationship between the wobble frequency of the stator ring and the frequency of rotation of the rotor ring in terms of support stiffness, moment of inertia and mean radius of the stator ring. It is suggested that the design of the seal should be done with an eye on condition (2.62), and  $k$  and  $I_o$  so chosen that, for the shaft speed dictated by the particular application, condition (2.62) is not fulfilled. Specifically, in order to avoid a case of exponential growth of  $r$  or a case of constant  $r$ , the condition,

$$\omega < \sqrt{\frac{8k r_m^2}{I_o}}$$

must be satisfied.

## APPENDIX A

### The Integral 'R'

$$R = \int_{r_i}^{r_o} (r^4 - (r_o + r_i)r^3 + r_o r_i r^2) dr = \left[ \frac{r^5}{5} - (r_o + r_i)\frac{r^4}{4} + r_o r_i \frac{r^3}{3} \right]_{r_i}^{r_o}$$

$$R = \frac{1}{5} (r_o^5 - r_i^5) - \frac{1}{4} (r_o + r_i) (r_o^4 - r_i^4) + \frac{1}{3} r_o r_i (r_o^3 - r_i^3) \quad (A1)$$

Where R is a negative constant.

### The Journal Bearing Integrals [7]

$$\begin{aligned} & \int_0^{2\pi} \frac{\cos \phi \sin (\phi - \psi t) d\phi}{[\bar{h} + \gamma r_m \cos (\phi - \psi t)]^3} = \int_0^{2\pi} \frac{\cos[(\phi - \psi t) + \psi t] \sin(\phi - \psi t) d\phi}{[\bar{h} + \gamma r_m \cos(\phi - \psi t)]^3} \\ &= \int_0^{2\pi} \left\{ \frac{\cos(\phi - \psi t) \sin(\phi - \psi t) \cos \psi t - \sin^2(\phi - \psi t) \sin \psi t}{[\bar{h} + \gamma r_m \cos(\phi - \psi t)]^3} \right\} d\phi \\ &= \cos \psi t \int_0^{2\pi} \frac{\sin(\phi - \psi t) \cos(\phi - \psi t)}{[\bar{h} + \gamma r_m \cos(\phi - \psi t)]^3} d\phi - \sin \psi t \int_0^{2\pi} \frac{\sin^2(\phi - \psi t) d\phi}{[\bar{h} + \gamma r_m \cos(\phi - \psi t)]^3} \\ & \int_0^{2\pi} \frac{\sin(\phi - \psi t) \cos(\phi - \psi t) d\phi}{[\bar{h} + \gamma r_m \cos(\phi - \psi t)]^3} = \frac{1}{\bar{h}^3} \int_0^{2\pi} \frac{\sin(\phi - \psi t) \cos(\phi - \psi t) d\phi}{[1 + \varepsilon \cos \phi]^3} = \frac{1}{\bar{h}^3} \left[ I_3'' \right]_0^{2\pi} \equiv -\frac{J_3^{11}}{\bar{h}^3} \end{aligned}$$

$$\text{where } \varepsilon = \frac{\gamma r_m}{\bar{h}}, \quad 0 < \varepsilon^2 \ll 1$$

$$I_3'' = \frac{1}{\varepsilon} \left[ -I_3^{10} + I_2^{10} \right]_0^{2\pi} = \frac{1}{\varepsilon} \left[ \frac{-1}{2\varepsilon(1+\varepsilon \cos(\phi - \psi t))^2} + \frac{1}{\varepsilon(1+\varepsilon \cos(\phi - \psi t))} \right]_0^{2\pi} = 0$$

Therefore

$$\int_0^{2\pi} \frac{\sin(\phi - \dot{\psi}t) \cos(\phi - \dot{\psi}t) d\phi}{[\bar{h} + \gamma r_m \cos(\phi - \dot{\psi}t)]^3} = 0 \quad (\text{A2})$$

$$\int_0^{2\pi} \frac{\sin^2(\phi - \dot{\psi}t) d\phi}{[\bar{h} + \gamma r_m \cos(\phi - \dot{\psi}t)]^3} = -\frac{1}{\bar{h}^3} \int_0^{2\pi} \frac{\sin^2(\phi - \dot{\psi}t) d\phi}{[1 + \epsilon \cos\phi]^3} \equiv -\frac{1}{\bar{h}^3} [I_s^{20}]_0^{2\pi} \equiv -\frac{J_s^{20}}{\bar{h}^3},$$

where  $J_s^{20} = \frac{1}{\epsilon^2} \left[ -(1-\epsilon^2) I_s^{\infty} + 2I_2^{\infty} - I_4^{\infty} \right]_0^{2\pi}$

$$I_s^{\infty} = \frac{1}{2(1-\epsilon^2)} \left[ \frac{-\epsilon \sin(\phi - \dot{\psi}t)}{(1+\epsilon \cos(\phi - \dot{\psi}t))^3} + 3I_2^{\infty} - I_4^{\infty} \right]_0^{2\pi}$$

Substituting for  $I_s^{\infty}$  in  $J_s^{20}$ ,

$$J_s^{\infty} = \frac{1}{\epsilon^2} \left\{ \frac{-1}{2} \left[ \frac{-\epsilon \sin(\phi - \dot{\psi}t)}{(1+\epsilon \cos(\phi - \dot{\psi}t))^2} + 3I_2^{\infty} - I_4^{\infty} \right] + 2I_2^{\infty} - I_4^{\infty} \right\}_0^{2\pi}$$

$$= \frac{1}{\epsilon^2} \left[ \frac{\epsilon \sin(\phi - \dot{\psi}t)}{2[1+\epsilon \cos(\phi - \dot{\psi}t)]^2} + \frac{1}{2} I_2^{\infty} - \frac{1}{2} I_4^{\infty} \right]_0^{2\pi}$$

$$= \frac{1}{2\epsilon^2} \left[ \frac{\epsilon \sin(\phi - \psi t)}{[1 + \epsilon \cos(\phi - \psi t)]^2} + I_2^\infty - I_1^\infty \right]_0^{2\pi}$$

where,  $I_2^\infty = \frac{1}{(1-\epsilon^2)} \left[ \frac{-\epsilon \sin(\phi - \psi t)}{1 + \epsilon \cos(\phi - \psi t)} + I_1^\infty \right]$

Substituting for  $I_2^\infty$  in  $J_s^{20}$

$$\begin{aligned} J_s^{20} &= \frac{1}{2\epsilon^2} \left[ \frac{\epsilon \sin(\phi - \psi t)}{[1 + \epsilon \cos(\phi - \psi t)]^2} - \frac{\epsilon \sin(\phi - \psi t)}{(1-\epsilon^2)(1 + \epsilon \cos(\phi - \psi t))} + I_1^\infty \left( \frac{1}{1-\epsilon^2} - 1 \right) \right]_0^{2\pi} \\ &= \frac{1}{(1-\epsilon^2)} \frac{\pi}{(1-\epsilon)^{1/2}} = \frac{\pi}{(1-\epsilon)^{3/2}} \end{aligned}$$

Therefore,

$$\int_0^{2\pi} \frac{\sin^2(\phi - \psi t) d\phi}{[\bar{h} + \gamma r_m \cos(\phi - \psi t)]^3} = \frac{\pi}{(1-\epsilon^2)^{3/2}}$$

for small  $\gamma$ ,  $\epsilon^2 \ll 1$ ,

Therefore,

$$\int_0^{2\pi} \frac{\sin^2(\phi - \dot{\psi}t) d\phi}{[\bar{h} + \gamma r_m \cos(\phi - \dot{\psi}t)]^3} = \pi \quad (\text{A3})$$

Thus,

$$\int_0^{2\pi} \frac{\cos\phi \sin(\phi - \dot{\psi}t) d\phi}{[\bar{h} + \gamma r_m \cos(\phi - \dot{\psi}t)]^3} = \frac{-3\mu\gamma r_m (2\dot{\psi} - \omega) R \pi \sin\dot{\psi}t}{\bar{h}^3} \quad (\text{A4})$$

$$\int_0^{2\pi} \frac{\sin\phi \sin(\phi - \dot{\psi}t) d\phi}{[\bar{h} + \gamma r_m \cos(\phi - \dot{\psi}t)]^3} = \int_0^{2\pi} \frac{\sin[(\phi - \dot{\psi}t) + \dot{\psi}t] \sin(\phi - \dot{\psi}t) d\phi}{[\bar{h} + \gamma r_m \cos(\phi - \dot{\psi}t)]^3}$$

$$= \int_0^{2\pi} \left\{ \frac{\sin^2(\phi - \dot{\psi}t) \cos\dot{\psi}t + \cos(\phi - \dot{\psi}t) \sin(\phi - \dot{\psi}t) \sin\dot{\psi}t}{[\bar{h} + \gamma r_m \cos(\phi - \dot{\psi}t)]^3} \right\} d\phi$$

$$= \cos\dot{\psi}t \int_0^{2\pi} \frac{\sin^2(\phi - \dot{\psi}t) d\phi}{[\bar{h} + \gamma r_m \cos(\phi - \dot{\psi}t)]^3} + \sin\dot{\psi}t \int_0^{2\pi} \frac{\sin(\phi - \dot{\psi}t) \cos(\phi - \dot{\psi}t) d\phi}{[\bar{h} + \gamma r_m \cos(\phi - \dot{\psi}t)]^3}$$

From (A2) and (A3)

$$\int_0^{2\pi} \frac{\sin\phi \sin(\phi - \dot{\psi}t) d\phi}{[\bar{h} + \gamma r_m \cos(\phi - \dot{\psi}t)]^3} = \frac{3\mu\gamma r_m (2\dot{\psi} - \omega) R \pi \cos\dot{\psi}t}{\bar{h}^3} \quad (\text{A5})$$

$$\int_0^{2\pi} \frac{\cos\phi \cos(\phi - \dot{\psi}t) d\phi}{[\bar{h} + \gamma r_m \cos(\phi - \dot{\psi}t)]^3} = \int_0^{2\pi} \frac{\cos[(\phi - \dot{\psi}t) + \dot{\psi}t] \cos(\phi - \dot{\psi}t) d\phi}{[\bar{h} + \gamma r_m \cos(\phi - \dot{\psi}t)]^3}$$

$$= \int_0^{2\pi} \left\{ \frac{\cos^2(\phi - \dot{\psi}t) \cos\dot{\psi}t - \sin(\phi - \dot{\psi}t) \cos(\phi - \dot{\psi}t) \sin\dot{\psi}t}{[\bar{h} + \gamma r_m \cos(\phi - \dot{\psi}t)]^3} \right\} d\phi$$

$$= \cos\dot{\psi}t \int_0^{2\pi} \frac{\cos^2(\phi - \dot{\psi}t) d\phi}{[\bar{h} + \gamma r_m \cos(\phi - \dot{\psi}t)]^3} - \sin\dot{\psi}t \int_0^{2\pi} \frac{\sin(\phi - \dot{\psi}t) \cos(\phi - \dot{\psi}t) d\phi}{[\bar{h} + \gamma r_m \cos(\phi - \dot{\psi}t)]^3}$$

$$\int_0^{2\pi} \frac{\cos^2(\phi - \dot{\psi}t) d\phi}{[\bar{h} + \gamma r_m \cos(\phi - \dot{\psi}t)]^3} = \frac{1}{\bar{h}^3} \int_0^{2\pi} \frac{\cos^2(\phi - \dot{\psi}t) d\phi}{[1 + \epsilon \cos(\phi - \dot{\psi}t)]^3} = \frac{1}{\bar{h}^3} \left[ I_s^{\infty} \right]_0^{2\pi} = \frac{J_s^{\infty}}{\bar{h}^3}$$

where  $J_s^{\infty} = \frac{1}{\epsilon^2} \left[ I_s^{\infty} - 2I_2^{\infty} + I_1^{\infty} \right]_0^{2\pi}$

$$= \frac{1}{\epsilon^2} \left\{ \left[ I_s^{\infty} \right]_0^{2\pi} - 2 \left[ I_2^{\infty} \right]_0^{2\pi} + \left[ I_1^{\infty} \right]_0^{2\pi} \right\}$$

$$I_s^{\infty} = \frac{1}{2(1-\epsilon^2)} \left[ \frac{-\epsilon \sin \phi}{[1+\epsilon \cos(\phi - \dot{\psi}t)]^2} + 3I_2^{\infty} - I_1^{\infty} \right]$$

$$I_2^{\infty} = \frac{1}{(1-\epsilon^2)} \left[ \frac{-\epsilon \sin(\phi - \dot{\psi}t)}{1+\epsilon \cos(\phi - \dot{\psi}t)} + I_1^{\infty} \right]$$

Substituting for  $I_2^{\infty}$  in  $I_s^{\infty}$ ,

$$I_s^{\infty} = \frac{1}{2(1-\epsilon^2)} \left[ \frac{-\epsilon \sin(\phi - \dot{\psi}t)}{[1+\epsilon \cos(\phi - \dot{\psi}t)]^2} + \frac{3}{(1-\epsilon^2)} \left[ \frac{-\epsilon \sin(\phi - \dot{\psi}t)}{1+\epsilon \cos(\phi - \dot{\psi}t)} + I_1^{\infty} \right] - I_1^{\infty} \right]$$

$$\left[ I_s^{\infty} \right]_0^{2\pi} = \frac{1}{2(1-\varepsilon^2)} \left[ \frac{3}{1-\varepsilon^2} - 1 \right] \frac{2\pi}{(1-\varepsilon^2)^{1/2}}$$

$$\left[ I_2^{\infty} \right]_0^{2\pi} = \frac{1}{(1-\varepsilon)^2} \frac{2\pi}{(1-\varepsilon^2)^{1/2}}$$

Substituting for  $\left[ I_s^{\infty} \right]_0^{2\pi}$  and  $\left[ I_2^{\infty} \right]_0^{2\pi}$  in  $J_s^{\infty}$ ,

$$J_s^{\infty} = \frac{1}{\varepsilon^2} \left[ \frac{\pi}{(1-\varepsilon^2)(1-\varepsilon^2)^{1/2}} \left( \frac{3}{1-\varepsilon^2} - 1 \right) - \frac{4\pi}{(1-\varepsilon^2)(1-\varepsilon^2)^{1/2}} + \frac{2\pi}{(1-\varepsilon^2)^{1/2}} \right]$$

$$= \frac{\pi}{\varepsilon^2 (1-\varepsilon^2)^{1/2}} \left[ \frac{1}{1-\varepsilon^2} \left( \frac{3}{1-\varepsilon^2} - 1 \right) + 2 - \frac{4}{1-\varepsilon^2} \right]$$

$$= \frac{\pi}{\varepsilon^2 (1-\varepsilon^2)^{3/2}} \left[ \frac{3}{1-\varepsilon^2} - 1 - 2 (1 + \varepsilon^2) \right]$$

$$= \frac{\pi}{\varepsilon^2 (1-\varepsilon^2)^{3/2}} \left[ \frac{2 + \varepsilon^2 - 2 (1 + \varepsilon^2)}{1-\varepsilon^2} \right]$$

$$= \frac{\pi (\varepsilon^2 + 2 \varepsilon^4)}{\varepsilon^2 (1 - \varepsilon^2)^{5/2}}$$

$$J_s^{\infty} = \frac{2\pi (1/2 + \varepsilon)^2}{(1 - \varepsilon^2)^{5/2}}$$

for small  $\gamma$ ,  $\gamma^2 \ll 1$ ,  $\varepsilon^2 \ll 1$ , therefore

$$J_s^{\infty} = \pi$$

Thus,

$$\int_0^{2\pi} \frac{\cos\phi \cos(\phi - \psi t) d\phi}{[\bar{h} + \gamma r_m \cos(\phi - \psi t)]^3} = \frac{6\pi\mu r_m R \cos\psi t}{\bar{h}^3} \quad (A6)$$

**APPENDIX B**

-----

(1) Comparison of complete and approx. values of hydrodynamic pressure

(A) Complete

-----

Theta(Degrees)	Pressure(Pa)
.0	.0
20.0	8989.54
40.0	17322.41
60.0	24259.39
80.0	28948.09
100.0	30497.0
120.0	28188.53
140.0	21803.05
160.0	11921.31
180.0	.0
200.0	-11921.31
220.0	-21803.05
240.0	-28188.53
260.0	-30497.0
280.0	-28948.0
300.0	-24259.4
320.0	-17322.41
340.0	-8989.54
360.0	.0

(B) Approximate

-----

.0	.0
20.0	8987.78
40.0	17318.81
60.0	24253.87
80.0	28940.78
100.0	30488.43
120.0	28179.86
140.0	21795.84
160.0	11917.19
180.0	.0
200.0	-11917.19
220.0	-21795.84
240.0	-28179.86
260.0	-30488.43
280.0	-28940.78
300.0	-24253.87
320.0	-17318.81
340.0	-8987.78
360.0	.0

(2) Comparison of complete and approximate values of squeeze pressure.

(A) Complete

Theta(Degrees)	Pressure(Pa)
.0	-66355.37
20.0	-62894.22
40.0	-52569.52
60.0	-35666.33
80.0	-12998.04
100.0	13693.51
120.0	41442.98
140.0	66167.21
160.0	83406.02
180.0	89607.18
200.0	83406.02
220.0	66167.21
240.0	41442.98
260.0	13693.51
280.0	-12998.04
300.0	-35666.33
320.0	-52569.52
340.0	-62894.22
360.0	-66355.37

(B) Approximate

.0	-66342.72
20.0	-62881.96
40.0	-52558.60
60.0	-35658.21
80.0	-12994.75
100.0	13689.67
120.0	41430.23
140.0	66145.35
160.0	83377.20
180.0	89575.73
200.0	83377.20
220.0	66145.35
240.0	41430.23
260.0	13689.67
280.0	-12994.75
300.0	-35658.21
320.0	-52558.60
340.0	-62881.96
360.0	-66342.72

## APPENDIX C

Solutions to the quartic equation,

$$\psi^4 + \left(\frac{A^2}{4} - B\right)\psi^2 - \left(\frac{A\omega}{4}\right)^2 = 0 \quad (C1)$$

The quartic equation of reference [8], has the form,

$$x^4 + ax^3 + bx^2 + cx + d = 0 \quad (C2)$$

Comparing equations (C1) and (C2), the coefficients are

$$a = 0$$

$$b = -\frac{A^2}{4} - B$$

$$c = 0$$

$$d = -\left(\frac{A\omega}{4}\right)^2 \quad (C3)$$

The resolvent cubic equation is of the form,

$$y^3 - by^2 + (ac - 4d)y - a^2d + 4bd - c^2 = 0 \quad (C4)$$

Substituting for the appropriate coefficients (C3), in equation (C4),

$$y^3 - \left(\frac{A^2}{4} - B\right)y^2 + \left(\frac{A\omega}{2}\right)^2 y - \left(\frac{A^2}{4} - B\right) \left(\frac{A\omega}{2}\right)^2 = 0$$

$$\text{i.e. } \left[y - \left(\frac{A^2}{4} - B\right)\right] \left(y^2 + \left(\frac{A\omega}{2}\right)^2\right) = 0 \quad (\text{C5})$$

One root of the resolvent cubic eqn (C4), required for solving the quartic equation is,

$$y = \frac{A\omega}{2} \quad (\text{C6})$$

Using the same nomenclature as given in the table being referred to, the required formulae are,

$$R = \sqrt{\frac{a^2}{4} - b + y}$$

$$D = \sqrt{\frac{3a^2}{4} - R^2 - 2b + \frac{4ab - 8c - a^3}{4R}}$$

$$E = \sqrt{\frac{3a^2}{4} - R^2 - 2b - \frac{4ab - 8c - a^3}{4R}} \quad (\text{C7})$$

Substituting the appropriate coefficients (C3), and one root of the resolvent cubic equation (C6), in the set of formulae (C7),

$$R = \sqrt{B - \frac{A^2}{4} + \frac{A\omega}{2}}$$

$$D = E = \sqrt{B - \frac{A\omega}{2} - \frac{A^2}{4}} \quad (C8)$$

The formulae that give the roots of the quartic equation are,

$$\frac{y}{z_{1,2}} = \frac{R}{2} \pm \frac{D}{2}$$

$$\frac{y}{z_{3,4}} = -\frac{R}{2} \pm \frac{E}{2} \quad (C9)$$

Substituting for D, E and R from equations (C8)

$$\frac{y}{z_{1,2}} = \frac{1}{2} \sqrt{B - \frac{A^2}{4} + \frac{A\omega}{2}} \pm \frac{1}{2} \sqrt{B - \frac{A^2}{4} - \frac{A\omega}{2}}$$

$$\frac{y}{z_{3,4}} = -\frac{1}{2} \sqrt{B - \frac{A^2}{4} + \frac{A\omega}{2}} \pm \frac{1}{2} \sqrt{B - \frac{A^2}{4} - \frac{A\omega}{2}} \quad (C10)$$

#### REFERENCES

1. Orcutt, F.K., "An Investigation of the Operation and Failure of Mechanical Face Seals" Journal of Lubrication Technology, ASME Trans., Ser. F, Vol. 91, Oct. 1969, pp.713-725.
2. Stanghan - Batch, B. and Iny, E.H., "A Hydrodynamic Theory of Radial - Face Mechanical Seals", Journal of Mechanical Engineering Science, Vol. 15, No.1, 1973.
3. Vygodsky, M., Mathematical Handbook, MIR Publishers, Moscow, 1975.
4. Meriam, J.L., Dynamics, John Wiley and Sons, Inc. Second Printing, July, 1966.
5. Etsion, I. and Burton, R.A., "Observation of Self-Excited Wobble in Face Seals' Journal of Lubrication Technology, ASME Trans., Vol. 101, Oct. 1979, pp.526-528.
6. Etsion, I., "Non-Axisymmetric Incompressible Hydrostatic Pressure Effects in Radial Face Seals", ASME Journal of Lubrication Technology, Vol. 100, No.3, July 1978, pp. 379.385.
7. Booker, J.F., A Table of the Journal-Bearing Integral ASME Journal of Basic Engineering, Vol. 87, June 1965, pp.533-535.
8. Beyer, W.H., (Ed.), CRC Standard Mathematical Tables 24th. edition.